Mirror quiescence and high-sensitivity position measurements with feedback

David Vitali,[1] Stefano Mancini,[1] Luciano Ribichini,[2] and Paolo Tombesi[1]
[1]*INFM, Dipartimento di Fisica, Università di Camerino, I-62032 Camerino, Italy*
[2]*Albert Einstein Institut für Gravitationsphysik, Aussenstelle Hannover, Callinstrasse 38, D-30167 Hannover, Germany*
(Received 12 November 2001; published 29 May 2002)

We present a detailed study of how phase-sensitive feedback schemes can be used to improve the performance of optomechanical devices. Considering the case of a cavity mode coupled to an oscillating mirror by the radiation pressure, we show how feedback can be used to reduce the position noise spectrum of the mirror, cool it to its quantum ground state, or achieve position squeezing. Then, we show that even though feedback is not able to improve the sensitivity of stationary position spectral measurements, it is possible to design a nonstationary strategy able to increase this sensitivity.

DOI: 10.1103/PhysRevA.65.063803 PACS number(s): 42.50.Lc, 03.65.Ta, 05.40.Jc, 04.80.Nn

I. INTRODUCTION

Mirrors play a crucial role in a variety of precision measurements such as gravitational wave detection [1] and atomic force microscopes [2]. In these applications one needs a very high resolution for position measurements and a good control of the various noise sources, because one has to detect the effect of a very weak force [3,4]. As shown by the pioneering work of Braginsky [5], even though all classical noise sources had been minimized, the detection of gravitational waves would be ultimately determined by quantum fluctuations and the Heisenberg uncertainty principle. Quantum noise in interferometers has two fundamental sources, the photon shot noise of the laser beam, prevailing at low laser intensity, and the fluctuations of the mirror position due to radiation pressure, which is proportional to the incident laser power. This radiation pressure noise is the so-called ''back-action noise'' arising from the fact that intensity fluctuations affect the momentum fluctuations of the mirror, which are then fed back into the position by the dynamics of the mirror. The two quantum noises are minimized at an optimal, intermediate, laser power, yielding the so-called *standard quantum limit* (SQL) [3,6]. Real devices constructed up to now are still far from the standard quantum limit because quantum noise is much smaller than that of classical origin, which is essentially given by thermal noise. In fact, present interferometric gravitational wave detectors are limited by the Brownian motion of the suspended mirrors [7], which can be decomposed into suspension and internal (i.e., of internal acoustic modes) thermal noise. Therefore it is very important to establish the experimental limitations determined by the thermal noise, and recent experiments [8,9] go in this direction.

Recently, Ref. [10] reported the first experimental evidence of the reduction of thermal noise by means of the radiation pressure of an appropriately modulated laser light incident on the back of the mirror [11]. The method was based on a phase-sensitive feedback control proposed in Ref. [12]: detect the mirror displacement through a homodyne measurement, and then use the output photocurrent to realize a real-time reduction of the mirror fluctuations. The proposed scheme is a sort of continuous version of the stochastic cooling technique used in accelerators [13], because the feedback continuously ''kicks'' the mirror in order to put it in its equilibrium position. This proposal has been experimentally realized in Ref. [11], using the ''cold damping'' technique [14], which amounts to applying a viscous feedback force to the oscillating mirror. In the experimental studies of optomechanical systems performed up to now, the effects of quantum noise are blurred by thermal noise and the experimental results can be well explained in classical terms (see, for example, [15]). However, developing a fully quantum description of the system in the presence of feedback is of fundamental importance for two main reasons. First of all it allows to establish the conditions under which the effects of quantum noise in optomechanical systems become visible and experimentally detectable. We have recently shown in Ref. [16] that there is an appreciable difference between the classical and quantum description of feedback already at liquid He temperatures. Moreover, a completely quantum treatment allows one to establish the ultimate limits of the proposed feedback schemes, as, for example, the possibility to reach the ground-state cooling of a mechanical, macroscopic degree of freedom. In Ref. [12], a quantum treatment of stochastic cooling feedback has been already presented, based, however, on a master-equation description which is not valid at very low temperatures [17]. A consistent quantum description of both stochastic cooling and cold damping feedback schemes, valid at all temperatures, has been presented in [16], and recently a discussion of the quantum limits of cold damping has been presented in [18]. The present paper will extend and generalize the results of [16,18], allowing us to make a detailed comparison of the two feedback schemes, and to establish all their potential applications. In particular, we shall see that both schemes can achieve ground-state cooling of an oscillating mode of the mirror, and that, in an appropriate limit, the ''stochastic cooling'' feedback of Ref. [12], can even break the standard quantum limit, achieving steady-state position squeezing. The experimental realization of these quantum limits in optomechanical systems is extremely difficult, but the feedback methods described in this paper may be useful also for microelectromechanical systems, where the search for quantum effects in mechanical systems is also very active [19,20].

Thermal noise reduction is important, but is not the only relevant aspect. What is more important, especially for gravi-

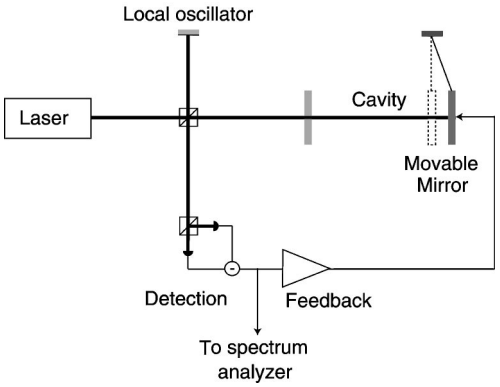

FIG. 1. Schematic description of the system. The cavity mode is driven by the laser which, thanks to the beam splitter, provides also the local oscillator for the homodyne measurement. The signal is then fed back to the mirror motion.

tational wave detection [1], or for metrology applications [20], is to improve the sensitivity, i.e., the signal-to-noise ratio (SNR) of position measurements [4]. Both the stochastic cooling scheme of Ref. [12] and the cold damping scheme of Ref. [11] cool the mirror by overdamping it, thereby strongly decreasing its mechanical susceptibility at resonance. Cooling is therefore achieved through the suppression of the resonance peak in the noise power spectrum. This suggests that both feedback schemes cannot be directly applied to improve the sensitivity for the detection of weak forces, because the strong reduction of the mechanical susceptibility at resonance means that the mirror does not respond both to the noise and to the signal. We shall see that this is true only in stationary conditions, i.e., we shall prove that the *stationary* spectral SNR is never improved by feedback. However, as we have recently shown in [16], it is possible to use feedback with an appropriate *nonstationary* strategy, able to increase significantly the SNR for the detection of *impulsive* classical forces acting on the oscillator. Here we shall extend the results of [16] by adopting a general description of nonstationary spectral measurements.

The outline of the paper is as follows. In Sec. II we describe the model and derive the appropriate quantum Langevin equations. In Sec. III we describe the stochastic cooling feedback scheme of Ref. [12] and the cold damping feedback using the quantum Langevin theory developed in [21,22], and we make a detailed comparison of the two schemes. In Sec. IV we analyze the stationary state of the oscillating mirror, and we determine the conditions under which feedback can be used to achieve ground-state cooling or position squeezing. In Sec. V we present a general description of nonstationary spectral measurement and we discuss the stationary limit in particular. Section VI describes how the sensitivity of position measurements can be improved by using feedback in a nonstationary way, and Sec. VII is for concluding remarks.

II. THE MODEL

The system studied in the present paper consists of a coherently driven optical cavity with a moving mirror (Fig. 1). This optomechanical system can represent one arm of an interferometer able to detect weak forces as those associated with gravitational waves [1], or an atomic force microscope [2]. The detection of very weak forces requires having quantum limited devices, whose sensitivity is ultimately determined by the quantum fluctuations. For this reason we shall describe the mirror as a single *quantum*-mechanical harmonic oscillator with mass m and frequency ω_m. Experimentally, the mirror motion is the result of the excitation of many vibrational modes, including internal acoustic modes. The description of the mirror as a single oscillator is, however, a good approximation when frequencies are limited to a bandwidth including a single mechanical resonance, by using, for example, a bandpass filter in the detection loop [23].

The optomechanical coupling between the mirror and the cavity field is realized by the radiation pressure. The electromagnetic field exerts a force on the movable mirror which is proportional to the intensity of the field, which, at the same time, is phase shifted by $2kq$, where k is the wave vector and q is the mirror displacement from the equilibrium position. In the adiabatic limit in which the mirror frequency is much smaller than the cavity-free spectral range $c/2L$ (L is the cavity length) [24], one can focus on one cavity mode only because photon scattering into other modes can be neglected, and one has the following Hamiltonian [25]:

$$H=\hbar\omega_c b^\dagger b+\hbar\omega_m(P^2+Q^2)-2\hbar G b^\dagger bQ + i\hbar E(b^\dagger e^{-i\omega_0 t}-be^{i\omega_0 t}), \tag{1}$$

where b is the cavity mode annihilation operator with optical frequency ω_c, and E describes the coherent input field with frequency $\omega_0\sim\omega_c$ driving the cavity. Moreover, Q and P are the dimensionless position and momentum operator of the movable mirror, with $[Q,P]=i/2$, and $G=(\omega_c/L)\sqrt{\hbar/2m\omega_m}$ is the coupling constant. Since we shall focus on the quantum and thermal noise of the system, we shall neglect all the technical sources of noise, i.e., we shall assume that the driving laser is stabilized in intensity and frequency. This means neglecting all the fluctuations of the complex parameter E. Including these supplementary noise sources is, however, quite straightforward and a detailed calculation of their effect is shown in Ref. [26]. Moreover, recent experiments have shown that classical laser noise can be made negligible in the relevant frequency range [8,9]. The adiabatic regime $\omega_m\ll c/2L$ we have assumed in Eq. (1) implies $\omega_m\ll\omega_c$, and therefore the generation of photons due to the Casimir effect, and also retardation and Doppler effects are completely negligible.

The dynamics of the system is not only determined by the Hamiltonian interaction (1), but also by the dissipative interaction with external degrees of freedom. The cavity mode is damped due to the photon leakage through the mirrors that couple the cavity mode with the continuum of the outside electromagnetic modes. For simplicity we assume that the movable mirror has perfect reflectivity and that transmission takes place through the other, ''fixed,'' mirror only. We indicate the photon decay rate at the fixed mirror by γ_c. Then, the quantity E is related to the input laser power $\wp$ by E

$=\sqrt{\wp\,\gamma_c/\hbar\omega_0}$. The mechanical oscillator, which may represent not only the center-of-mass degree of freedom of the mirror, but also a torsional degree of freedom as in [9], or an internal acoustic mode as in [8], undergoes Brownian motion caused by the uncontrolled coupling with other internal and external modes at thermal equilibrium.

The dynamics of the system can be described by the following set of coupled quantum Langevin equations (QLE) (in the interaction picture with respect to $\hbar\omega_0 b^\dagger b$):

$$\dot{Q}(t)=\omega_m P(t), \tag{2a}$$

$$\dot{P}(t)=-\omega_m Q(t)+\mathcal{W}(t)-\gamma_m P(t)+G b^\dagger(t)b(t), \tag{2b}$$

$$\dot{b}(t)=-\left(i\omega_c-i\omega_0+\frac{\gamma_c}{2}\right)b(t)+2iGQ(t)b(t)+E+\sqrt{\gamma_c}b_{in}(t), \tag{2c}$$

where $b_{in}(t)$ is the input noise operator [27] associated with the vacuum fluctuations of the continuum of modes outside the cavity, having the following correlation functions:

$$\langle b_{in}(t)b_{in}(t')\rangle=\langle b_{in}^\dagger(t)b_{in}(t')\rangle=0, \tag{3a}$$

$$\langle b_{in}(t)b_{in}^\dagger(t')\rangle=\delta(t-t'). \tag{3b}$$

Furthermore, $\mathcal{W}(t)$ is the Brownian noise operator defined consistently with quantum mechanics [17]. It has the following correlation functions:

$$\langle \mathcal{W}(t)\mathcal{W}(t')\rangle=\frac{1}{2\pi}\frac{\gamma_m}{\omega_m}\{\mathcal{F}_r(t-t')+i\mathcal{F}_i(t-t')\}, \tag{4}$$

where

$$\mathcal{F}_r(t)=\int_0^{\varpi} d\omega\,\omega\cos(\omega t)\coth\left(\frac{\hbar\omega}{2k_BT}\right), \tag{5a}$$

$$\mathcal{F}_i(t)=-\int_0^{\varpi} d\omega\,\omega\sin(\omega t), \tag{5b}$$

with T the bath temperature, γ_m the mechanical decay rate, k_B the Boltzmann constant, and ϖ the frequency cutoff of the reservoir spectrum. The antisymmetric part, $\mathcal{F}_i$, of Eq. (4) is a direct consequence of the commutation relations for the Brownian noise operator, and the symmetric part, $\mathcal{F}_r$ explicitly depends on temperature and becomes proportional to a Dirac δ function when the high-temperature limit $k_BT\gg\hbar\varpi$ first, and the infinite frequency cutoff limit $\varpi\to\infty$ later, are taken. Equations (4) and (5) show the non-Markovian nature of quantum Brownian motion, which becomes particularly evident in the low-temperature limit [28,29]. Therefore, the *exact* QLE (2) reduce to the standard ones [27] in the limit $\varpi\to\infty$. It is also important to stress that the quantum Langevin description of quantum Brownian motion given by Eq. (2) is more general than that associated with a master-equation approach, because it is valid *at all temperatures* and it does not need any high-temperature limit [17].

In standard interferometric applications, the driving field is very intense. Under this condition, the system is characterized by a semiclassical steady state with the internal cavity mode in a coherent state $|\beta\rangle$, and a new equilibrium position for the mirror, displaced by $G|\beta|^2/\omega_m$ with respect to that with no driving field. The steady-state amplitude is given by the solution of the nonlinear equation

$$\beta=\frac{E}{\frac{\gamma_c}{2}+i\omega_c-i\omega_0-2i\frac{G^2}{\omega_m}|\beta|^2}, \tag{6}$$

which is obtained by taking the expectation values of Eqs. (2), factorizing them and setting all the time derivatives to zero. Equation (6) shows a bistable behavior that has been experimentally observed in [30]. Under these semiclassical conditions, the dynamics is well described by linearizing the QLE (2) around the steady state. If we now rename with $Q(t)$ and $b(t)$ the operators describing the quantum fluctuations around the classical steady state, we get

$$\dot{Q}(t)=\omega_m P(t), \tag{7a}$$

$$\dot{P}(t)=-\omega_m Q(t)-\gamma_m P(t)+G\beta[b(t)+b^\dagger(t)]+\mathcal{W}(t), \tag{7b}$$

$$\dot{b}(t)=-\left(\frac{\gamma_c}{2}+i\Delta\right)b(t)+2iG\beta Q(t)+\sqrt{\gamma_c}b_{in}(t), \tag{7c}$$

where we have chosen the phase of the cavity mode field so that β is real and

$$\Delta=\omega_c-\omega_0-\frac{2G^2}{\omega_m}\beta^2 \tag{8}$$

is the cavity mode detuning. We shall consider from now on $\Delta=0$, which corresponds to the most common experimental situation, and which can always be achieved by appropriately adjusting the driving field frequency ω_0. In this case the dynamics becomes simpler, and, introducing the field phase quadrature $Y(t)=i(b^\dagger(t)-b(t))/2$ and field amplitude quadrature $X(t)=[b(t)+b^\dagger(t)]/2$, one has that only the phase quadrature $Y(t)$ is affected by the mirror position fluctuations $Q(t)$, while the amplitude field quadrature $X(t)$ is not. In fact, the linearized QLE (7) can be rewritten as

$$\dot{Q}(t)=\omega_m P(t), \tag{9a}$$

$$\dot{P}(t)=-\omega_m Q(t)-\gamma_m P(t)+2G\beta X(t)+\mathcal{W}(t), \tag{9b}$$

$$\dot{Y}(t)=-\frac{\gamma_c}{2}Y(t)+2G\beta Q(t)+\frac{\sqrt{\gamma_c}}{2}Y_{in}(t), \tag{9c}$$

$$\dot{X}(t)=-\frac{\gamma_c}{2}X(t)+\frac{\sqrt{\gamma_c}}{2}X_{in}(t), \tag{9d}$$

where we have introduced the phase input noise $Y_{in}(t) = i(b_{in}^{\dagger}(t) - b_{in}(t))$ and the amplitude input noise $X_{in}(t) = b_{in}^{\dagger}(t) + b_{in}(t)$.

III. POSITION MEASUREMENT AND FEEDBACK

Usually the movable mirror is used as a ponderomotive meter to detect small forces acting on it [6]. Thus, we introduce an additional Hamiltonian term describing the action of a classical external force $f(t)$, that is

$$H_{ext} = -Qf(t). \tag{10}$$

Information about such a force can be obtained by looking at the mechanical oscillator position $Q(t)$. The position measurement is commonly performed in the large cavity bandwidth limit $\gamma_c \gg G\beta,\ \omega_m$, when the cavity mode dynamics adiabatically follows that of the movable mirror and it can be eliminated, that is, from Eq. (9c),

$$Y(t) \simeq \frac{4G\beta}{\gamma_c} Q(t) + \frac{Y_{in}(t)}{\sqrt{\gamma_c}}, \tag{11}$$

and $X(t) \simeq X_{in}(t)/\sqrt{\gamma_c}$ from Eq. (9d). Performing a continuous homodyne measurement of the phase quadrature $Y(t)$ means, therefore, continuously monitoring the real-time dynamics of the oscillator position $Q(t)$, which, in turn, implies detecting the effects of classical force $f(t)$. The experimentally detected quantity is the output homodyne photocurrent [21,22,31]

$$Y_{out}(t) = 2\eta\sqrt{\gamma_c} Y(t) - \sqrt{\eta} Y_{in}^{\eta}(t), \tag{12}$$

where η is the detection efficiency and $Y_{in}^{\eta}(t)$ is a *generalized phase input noise*, coinciding with the input noise $Y_{in}(t)$ in the case of perfect detection $\eta = 1$, and taking into account the additional noise due to the inefficient detection in the general case $\eta < 1$ [22]. This generalized phase input noise can be written in terms of a generalized input noise $b_{\eta}(t)$ as $Y_{in}^{\eta}(t) = i(b_{\eta}^{\dagger}(t) - b_{\eta}(t))$. The quantum noise $b_{\eta}(t)$ is correlated with the input noise $b_{in}(t)$ and it is characterized by the following correlation functions [22]:

$$\langle b_{\eta}(t) b_{\eta}(t') \rangle = \langle b_{\eta}^{\dagger}(t) b_{\eta}(t') \rangle = 0, \tag{13a}$$

$$\langle b_{\eta}(t) b_{\eta}^{\dagger}(t') \rangle = \delta(t - t'), \tag{13b}$$

$$\langle b_{in}(t) b_{\eta}^{\dagger}(t') \rangle = \langle b_{\eta}(t) b_{in}^{\dagger}(t') \rangle = \sqrt{\eta}\,\delta(t - t'). \tag{13c}$$

The output of the homodyne measurement may be used to devise a phase-sensitive feedback loop to control the dynamics of the mirror. For example, we have proposed in Ref. [12] to reduce the effects of thermal noise on the mirror by feeding back the output homodyne photocurrent in an appropriate way. The proposed scheme is a sort of continuous version of the stochastic cooling technique used in accelerators [13], because the homodyne measurement provides a continuous monitoring of the oscillator's position, and the feedback continuously "kicks" the mirror in order to put it in its equilibrium position. Our proposal of cooling the mirror using a feedback loop has been experimentally realized in Ref. [11] (see also [15]), using a different method, the so-called "cold damping" technique [14]. This latter feedback scheme shares some analogies with that proposed in Ref. [12] and amounts to applying a viscous feedback force to the oscillating mirror. In the experiment of Refs. [11,15], the viscous force is provided by the radiation pressure of another laser beam, intensity modulated by the time derivative of the homodyne signal.

The effect of the feedback loop has been described using quantum trajectory theory [32] and the master-equation formalism in Ref. [12], and a classical description neglecting all quantum fluctuations in Ref. [11,15]. Here we shall use a more general description of feedback based on QLEs for Heisenberg operators, first developed in Ref. [21] and generalized to the nonideal detection case in Ref. [22] (see also [33] for a comparison between these quantum feedback approaches and general quantum control theories). This general quantum description of feedback will allow us to compare the two different feedback schemes, the stochastic cooling scheme of Ref. [12], and the cold damping scheme of Ref. [11,15]. A recent analysis of the quantum limits of cold damping has been presented in Ref. [18]. The present quantum treatment will also allow us to show that in the presence of feedback the radiation quantum noise has important effects, and that a classical stochastic treatment of the dynamics of the system is generally inadequate. Our treatment explicitly includes the limitations due to the quantum efficiency of the detection, but neglects other possible technical imperfections of the feedback loop, as, for example, the electronic noise of the feedback loop (discussed in [15]), or the fluctuations of the laser beam used for the feedback in the cold damping scheme.

A. Stochastic cooling

Let us first consider the stochastic cooling scheme of Ref. [12]. In this scheme, the feedback loop induces a continuous position shift controlled by the output homodyne photocurrent $Y_{out}(t)$. This effect of feedback manifests itself in an additional term in the QLE for a generic operator $\mathcal{O}(t)$ given by [22]

$$\dot{\mathcal{O}}_{fb}(t) = i\frac{\sqrt{\gamma_c}}{\eta} Y_{out}(t-\tau)[g_{sc} P(t), \mathcal{O}(t)], \tag{14}$$

where τ is the feedback loop delay time, and g_{sc} is a dimensionless feedback gain factor. The feedback delay time is essentially determined by the electronics involved in the feedback loop and is always much smaller than the typical time scale of the mirror dynamics. It is therefore common to consider the zero delay-time limit, $\tau \to 0$. This limit is, however, quite delicate in general [21,22]. In fact, $Y_{out}(t-\tau)$, being an output operator, commutes with $[g_{sc} P(t), \mathcal{O}(t)]$ for any nonzero τ, but this is no more true when $\tau = 0$. Therefore, one has to be careful with ordering in the zero delay-time limit. However, with the choice of Eq. (14) for the feedback term, the only nonzero commutator in the QLE of Eq. (9) is $[g_{sc} P(t), Q(t)]$, which, being a c number, does not

create any ordering ambiguity. Therefore one has exactly the same equations one would have by putting directly $\tau=0$ in Eq. (14), that is,

$$\dot{Q}(t)=\omega_m P(t)+g_{sc}\gamma_c Y(t)-\frac{g_{sc}}{2}\sqrt{\frac{\gamma_c}{\eta}}Y_{in}^{\eta}(t), \quad (15a)$$

$$\dot{P}(t)=-\omega_m Q(t)-\gamma_m P(t)+2G\beta X(t)+\mathcal{W}(t)+f(t), \quad (15b)$$

$$\dot{Y}(t)=-\frac{\gamma_c}{2}Y(t)+2G\beta Q(t)+\frac{\sqrt{\gamma_c}}{2}Y_{in}(t), \quad (15c)$$

$$\dot{X}(t)=-\frac{\gamma_c}{2}X(t)+\frac{\sqrt{\gamma_c}}{2}X_{in}(t), \quad (15d)$$

where we have used Eq. (12). After the adiabatic elimination of the radiation mode [see Eq. (11)], the above equations reduce to

$$\dot{Q}(t)=\omega_m P(t)+4G\beta g_{sc}Q(t)+\sqrt{\gamma_c}g_{sc}Y_{in}(t)-\frac{g_{sc}}{2}\sqrt{\frac{\gamma_c}{\eta}}Y_{in}^{\eta}(t), \quad (16a)$$

$$\dot{P}(t)=-\omega_m Q(t)-\gamma_m P(t)+\frac{2G\beta}{\sqrt{\gamma_c}}X_{in}(t)+\mathcal{W}(t)+f(t). \quad (16b)$$

The solution of these QLE for the conjugate operators $Q(t)$ and $P(t)$ can be easily obtained by performing the Laplace transform, and they will be useful in the following. Their expression is

$$Q(t)=K_Q(t)Q(0)+\chi_{sc}(t)P(0)+\int_0^t dt'\,\chi_{sc}(t')f(t-t')+\int_0^t dt'\;K_Q(t')\Big[\sqrt{\gamma_c}g_{sc}Y_{in}(t-t')-\frac{g_{sc}}{2}\sqrt{\frac{\gamma_c}{\eta}}Y_{in}^{\eta}(t-t')\Big]+\int_0^t dt'\;\chi_{sc}(t')\left[\mathcal{W}(t-t')+\frac{2G\beta}{\sqrt{\gamma_c}}X_{in}(t-t')\right], \quad (17a)$$

$$P(t)=K_P(t)P(0)-\chi_{sc}(t)Q(0)+\int_0^t dt'K_P(t')f(t-t')-\int_0^t dt'\;\chi_{sc}(t')\Big[\sqrt{\gamma_c}g_{sc}Y_{in}(t-t')-\frac{g_{sc}}{2}\sqrt{\frac{\gamma_c}{\eta}}Y_{in}^{\eta}(t-t')\Big]+\int_0^t dt'\;K_P(t')\left[\mathcal{W}(t-t')+\frac{2G\beta}{\sqrt{\gamma_c}}X_{in}(t-t')\right]. \quad (17b)$$

We have introduced the time-dependent susceptibility $\chi_{sc}(t)$ describing the response of the movable mirror in the presence of the stochastic cooling feedback

$$\chi_{sc}(t)=\frac{\omega_m}{\sqrt{\omega_m^2-\gamma_m^2\left(\frac{1-g_1}{2}\right)^2}}\times e^{-(1+g_1)\gamma_m t/2}\sin\left[t\sqrt{\omega_m^2-\gamma_m^2\left(\frac{1-g_1}{2}\right)^2}\right], \quad (18)$$

and the two related response functions

$$K_Q(t)=\frac{\dot{\chi}_{sc}(t)+\gamma_m\chi_{sc}(t)}{\omega_m}, \quad (19)$$

$$K_P(t)=\frac{\dot{\chi}_{sc}(t)+g_1\chi_{sc}(t)}{\omega_m}. \quad (20)$$

We have also rescaled the feedback gain and defined $g_1=-4G\beta g_{sc}/\gamma_m$.

B. Cold damping

Cold damping techniques, that is, the possibility to use a feedback loop to reduce the effective temperature of a system well below the operating temperature, have been applied in classical electromechanical systems for many years [14], and only recently they have been proposed to improve cooling and sensitivity at the quantum level [34]. This technique is based on the application of a negative derivative feedback, which increases the damping of the system without correspondingly increasing the thermal noise [14,34]. This technique has been successfully applied for the first time to an optomechanical system composed of a high-finesse cavity with a movable mirror in the experiments of Refs. [11,15]. In these experiments, the displacement of the mirror is measured with very high sensitivity [8], and the obtained information is fed back to the mirror via the radiation pressure of another, intensity-modulated, laser beam incident on the back of the mirror. Cold damping is obtained by modulating with the *time derivative* of the homodyne signal, in such a way that the radiation pressure force is proportional to the mirror

velocity. The servo-control force then corresponds to a viscous force. The results of Refs. [11,15] referred to a room-temperature experiment, and have been explained using a classical description. The quantum description of cold damping in this optomechanical system has been presented in [16] (see also Ref. [34]), and we shall follow this treatment.

In the quantum Langevin description, cold damping feedback scheme implies the following additional term in the QLE for a generic operator $\mathcal{O}(t)$ [16]:

$$\dot{\mathcal{O}}_{fb}(t)=\frac{i}{\eta\sqrt{\gamma_c}}\dot{Y}_{out}(t-\tau)[g_{cd}Q(t),\mathcal{O}(t)]. \tag{21}$$

As for the stochastic cooling feedback case, one has only one nonzero feedback term in the QLE of the system (9), which in this case is $[g_{cd}Q(t),P(t)]$. Since this commutator is a c number also in this case, we do not have any ordering problem in the zero delay-time limit, and the QLE for the cold damping feedback scheme becomes

$$\dot{Q}(t)=\omega_m P(t), \tag{22a}$$

$$\dot{P}(t)=-\omega_m Q(t)-\gamma_m P(t)+2G\beta X(t)-g_{cd}\dot{Y}(t)+\frac{g_{cd}}{2\sqrt{\gamma_c\eta}}\dot{Y}^{\eta}_{in}(t)+\mathcal{W}(t)+f(t), \tag{22b}$$

$$\dot{Y}(t)=-\frac{\gamma_c}{2}Y(t)+2G\beta Q(t)+\frac{\sqrt{\gamma_c}}{2}Y_{in}(t), \tag{22c}$$

$$\dot{X}(t)=-\frac{\gamma_c}{2}X(t)+\frac{\sqrt{\gamma_c}}{2}X_{in}(t). \tag{22d}$$

Adiabatically eliminating the cavity mode, one has

$$\dot{Q}(t)=\omega_m P(t), \tag{23a}$$

$$\dot{P}(t)=-\omega_m Q(t)-\gamma_m P(t)+\frac{2G\beta}{\sqrt{\gamma_c}}X_{in}(t)+\mathcal{W}(t)+f(t)-\frac{4G\beta g_{cd}}{\gamma_c}\dot{Q}(t)-\frac{g_{cd}}{\sqrt{\gamma_c}}\dot{Y}_{in}(t)+\frac{g_{cd}}{2\sqrt{\gamma_c\eta}}\dot{Y}^{\eta}_{in}(t). \tag{23b}$$

Notice that the modulation with the derivative of the homodyne photocurrent implies the introduction of two new quantum input noises, $\dot{Y}_{in}(t)$ and $\dot{Y}^{\eta}_{in}(t)$, whose correlation functions can be simply obtained by differentiating the corresponding correlation functions of $Y_{in}(t)$ and $Y^{\eta}_{in}(t)$. We have, therefore,

$$\langle\dot{Y}_{in}(t)\dot{Y}_{in}(t')\rangle=\langle\dot{Y}_{in}(t')\dot{Y}_{in}(t)\rangle=\langle\dot{Y}^{\eta}_{in}(t)\dot{Y}^{\eta}_{in}(t')\rangle=\langle\dot{Y}^{\eta}_{in}(t')\dot{Y}^{\eta}_{in}(t)\rangle=-\ddot{\delta}(t-t'), \tag{24a}$$

$$\langle\dot{Y}^{\eta}_{in}(t)\dot{Y}_{in}(t')\rangle=\langle\dot{Y}_{in}(t')\dot{Y}^{\eta}_{in}(t)\rangle=-\sqrt{\eta}\ddot{\delta}(t-t'), \tag{24b}$$

$$\langle X_{in}(t)\dot{Y}^{\eta}_{in}(t')\rangle=-\langle\dot{Y}^{\eta}_{in}(t')X_{in}(t)\rangle=-i\sqrt{\eta}\dot{\delta}(t-t'). \tag{24c}$$

In this case the solution of the adiabatic QLE reads

$$Q(t)=K(t)Q(0)+\chi_{cd}(t)P(0)+\int_0^t dt'\,\chi_{cd}(t')f(t-t')+\int_0^t dt'\,\chi_{cd}(t-t')\left[\frac{2G\beta}{\sqrt{\gamma_c}}X_{in}(t')+\mathcal{W}(t')-\frac{g_{cd}}{\sqrt{\gamma_c}}\dot{Y}_{in}(t')+\frac{g_{cd}}{2\sqrt{\gamma_c\eta}}\dot{Y}^{\eta}_{in}(t')\right], \tag{25}$$

and $P(t)=\dot{Q}(t)/\omega_m$, where we have introduced the time-dependent susceptibility in the case of the cold damping feedback scheme

$$\chi_{cd}(t)=\frac{\omega_m}{\sqrt{\omega_m^2-\gamma_m^2\left(\frac{1+g_2}{2}\right)^2}}\times e^{-(1+g_2)\gamma_m t/2}\sin\left[t\sqrt{\omega_m^2-\gamma_m^2\left(\frac{1+g_2}{2}\right)^2}\right] \tag{26}$$

and the related response function

$$K(t)=1-\omega_m\int_0^t dt'\,\chi_{cd}(t'). \tag{27}$$

We have again rescaled the feedback gain and defined $g_2=4G\beta\omega_m g_{cd}/\gamma_m\gamma_c$.

C. Comparison between the two feedback schemes

The two sets of QLE for the mirror Heisenberg operators, Eqs. (16) and (23), show that the two feedback schemes are not exactly equivalent. They are, however, physically analogous, as it can be seen, for example, by looking at the differential equation for the displacement operator $Q(t)$. In fact, from Eqs. (16) one gets

$$\ddot{Q}(t)+(1+g_1)\gamma_m\dot{Q}(t)+(\omega_m^2+\gamma_m^2 g_1)Q(t)=\omega_m\left[\frac{2G\beta}{\sqrt{\gamma_c}}X_{in}(t)+\mathcal{W}(t)+f(t)\right]+\sqrt{\gamma_c}g_{sc}\dot{Y}_{in}(t)-\frac{g_{sc}}{2}\sqrt{\frac{\gamma_c}{\eta}}\dot{Y}^{\eta}_{in}(t)+\frac{\gamma_m}{\omega_m}\left[\sqrt{\gamma_c}g_{sc}Y_{in}(t)-\frac{g_{sc}}{2}\sqrt{\frac{\gamma_c}{\eta}}Y^{\eta}_{in}(t)\right], \tag{28}$$

for the stochastic cooling scheme, while from Eqs. (23) one gets

$$\ddot{Q}(t)+(1+g_2)\gamma_m\dot{Q}(t)+\omega_m^2 Q(t) = \omega_m\left[\frac{2G\beta}{\sqrt{\gamma_c}}X_{in}(t)+\mathcal{W}(t)+f(t)-\frac{g_{cd}}{\sqrt{\gamma_c}}\dot{Y}_{in}(t) + \frac{g_{cd}}{2\sqrt{\gamma_c\eta}}\dot{Y}^{\eta}_{in}(t)\right] \tag{29}$$

for the cold damping scheme. These equations show that in both schemes the main effect of feedback is the modification of mechanical damping $\gamma_m \to \gamma_m(1+g_i)$ $(i=1,2)$. In the stochastic cooling scheme one has also a frequency renormalization $\omega_m^2 \to \omega_m^2+\gamma_m^2 g_1$, which is, however, usually negligible since the mechanical quality factor $\mathcal{Q}=\omega_m/\gamma_m$ is always large. Moreover, in the two cases the position dynamics is affected by similar, even though not identical, noise terms. This comparison shows that the stochastic cooling scheme of Ref. [12] is also able to provide a cold damping effect of increased damping without an increased temperature [16].

IV. STATIONARY STATE AND COOLING

We now study the stationary state of the movable mirror in the presence of the two feedback schemes, which is obtained by considering the dynamics in the asymptotic limit $t\to\infty$. We shall see that both feedback schemes are able to lower the effective temperature of the system, and that, in particular limits, the steady state can have interesting quantum features. In fact, both schemes are able to achieve ground-state cooling, and the stochastic cooling feedback is even able to achieve steady-state position squeezing.

A. Stochastic cooling feedback

Using the solution (17a), one has

$$\langle Q^2\rangle_{st} = \lim_{t\to\infty}\langle Q(t)^2\rangle = \int_0^\infty dt' \int_0^\infty dt'' K_Q(t')K_Q(t'')c_1(t'-t'') + \int_0^\infty dt' \int_0^\infty dt'' \chi_{sc}(t')\chi_{sc}(t'')c_2(t'-t''), \tag{30}$$

where $c_1(t)$ is the stationary symmetrized correlation function of the noise term $n_1(t)=\sqrt{\gamma_c}g_{sc}Y_{in}(t) - g_{sc}/2\sqrt{(\gamma_c/\eta)}Y^{\eta}_{in}(t)$, $c_2(t)$ is the stationary symmetrized correlation function of the noise term $n_2(t)=\mathcal{W}(t) + (2G\beta/\sqrt{\gamma_c})X_{in}(t)$, and we have used the fact that $n_1(t)$ and $n_2(t)$ are uncorrelated. Using the correlation functions (3), (4), and (13), one gets

$$c_1(t)=\frac{\gamma_c\gamma_m^2 g_1^2}{64\eta G^2\beta^2}\delta(t) \tag{31a}$$

$$c_2(t)=\frac{4G^2\beta^2}{\gamma_c}\delta(t)+\frac{\gamma_m}{2\pi\omega_m}\mathcal{F}_r(t). \tag{31b}$$

The expression for $\langle Q^2\rangle_{st}$ is obtained using Eqs. (18), (19), and (31) in Eq. (30),

$$\langle Q^2\rangle_{st}=\frac{\gamma_c\gamma_m g_1^2}{128\eta G^2\beta^2}\frac{1+\mathcal{Q}^2+g_1}{(1+g_1)(\mathcal{Q}^2+g_1)} + \frac{2G^2\beta^2}{\gamma_c\gamma_m}\frac{\mathcal{Q}^2}{(1+g_1)(\mathcal{Q}^2+g_1)}+\langle Q^2\rangle_{BM}. \tag{32}$$

The term $\langle Q^2\rangle_{BM}$ is the contribution of the mirror quantum Brownian motion, whose general expression is obtained by rewriting $\mathcal{F}_r(t'-t'')$ in Eq. (30) in terms of its Fourier transform $\mathcal{F}_r(\omega)$ [see Eq. (4)], to get

$$\langle Q^2\rangle_{BM}=\int_{-\varpi}^{\varpi}\frac{d\omega}{2\pi}\frac{\gamma_m}{2\omega_m}\omega\coth\left(\frac{\hbar\omega}{2k_BT}\right)|\tilde{\chi}_{sc}(\omega)|^2, \tag{33}$$

where

$$\tilde{\chi}_{sc}(\omega)=\frac{\omega_m}{\omega_m^2+g_1\gamma_m^2-\omega^2+i\omega\gamma_m(1+g_1)} \tag{34}$$

is the frequency-dependent susceptibility of the mirror in the stochastic cooling feedback scheme. The general analytical expression of the quantum Brownian motion term $\langle Q^2\rangle_{BM}$, valid in any range of parameters, is cumbersome and has been obtained in [28,29]. However, in typical optomechanical experiments [8,9,11,15] it is always $\hbar\gamma_m \ll \hbar\omega_m \ll k_BT$, and it is possible to see [28] that, in this limiting case, the classical approximation $\coth(\hbar\omega/2k_BT)\simeq 2k_BT/\hbar\omega$ [which is equivalent to approximate $\mathcal{F}_r(t)\simeq(\gamma_m k_BT/\hbar\omega_m)\delta(t)$] can be safely used in Eq. (33), so to get

$$\langle Q^2\rangle_{BM}=\frac{k_BT}{2\hbar\omega_m}\frac{\mathcal{Q}^2}{(1+g_1)(\mathcal{Q}^2+g_1)}. \tag{35}$$

Finally it is

$$\langle Q^2\rangle_{st}=\frac{g_1^2}{8\eta\zeta}\frac{1+\mathcal{Q}^2+g_1}{(1+g_1)(\mathcal{Q}^2+g_1)} + \left[\frac{\zeta}{8}+\frac{k_BT}{2\hbar\omega_m}\right]\frac{\mathcal{Q}^2}{(1+g_1)(\mathcal{Q}^2+g_1)}, \tag{36}$$

where we have introduced the rescaled, dimensionless, input power of the driving laser

$$\zeta=\frac{16G^2\beta^2}{\gamma_m\gamma_c}=\frac{64G^2}{\hbar\omega_0\gamma_m\gamma_c^2}\wp. \tag{37}$$

Equation (36) coincides with the corresponding one obtained in [12] using a master-equation description of the stochastic cooling feedback scheme.

An analogous procedure can be followed to get the stationary value $\langle P^2\rangle_{st}$. Using Eqs. (17b), (18), (20), (31), and (37), one obtains the general expression

$$\langle P^2\rangle_{st}=\frac{g_1^2}{8\eta\zeta}\frac{\mathcal{Q}^2}{(1+g_1)(\mathcal{Q}^2+g_1)}+\frac{\zeta}{8}\frac{g_1^2+\mathcal{Q}^2+g_1}{(1+g_1)(\mathcal{Q}^2+g_1)}+\langle P^2\rangle_{BM}, \tag{38}$$

where the quantum Brownian motion contribution is now given by

$$\langle P^2\rangle_{BM}=\int_{-\varpi}^{\varpi}\frac{d\omega}{2\pi}\frac{\gamma_m}{2\omega_m}\omega\coth\left(\frac{\hbar\omega}{2k_BT}\right)|\tilde{\chi}_{sc}(\omega)|^2\times\left(\frac{\omega^2+\gamma_m^2g_1^2}{\omega_m^2}\right). \tag{39}$$

In this case, the classical, high-temperature, approximation $\coth(\hbar\omega/2k_BT)\simeq 2k_BT/\hbar\omega$ has to be made with care, because, due to the presence of the ω^2 term, the integral (39) has an ultraviolet divergence in the usually considered $\varpi\to\infty$ limit [see also Eq. (34)]. This means that, differently from $\langle Q^2\rangle_{BM}$, the classical approximation for $\langle P^2\rangle_{BM}$ is valid only under the *stronger* condition $\hbar\varpi\ll k_BT$ [28], and that in the intermediate temperature range $\hbar\varpi\gg k_BT\gg\hbar\omega_m$ (which may be of interest for optomechanical systems), one has a correction of order $\ln(\hbar\varpi/k_BT)$. One has therefore [28]

$$\langle P^2\rangle_{BM}=\frac{k_BT}{2\hbar\omega_m}\frac{g_1^2+\mathcal{Q}^2+g_1}{(1+g_1)(\mathcal{Q}^2+g_1)}+\frac{\gamma_m}{\pi\omega_m}\ln\left(\frac{\hbar\varpi}{2\pi kT}\right), \tag{40}$$

so that one finally gets

$$\langle P^2\rangle_{st}=\frac{g_1^2}{8\eta\zeta}\frac{\mathcal{Q}^2}{(1+g_1)(\mathcal{Q}^2+g_1)}+\left[\frac{\zeta}{8}+\frac{k_BT}{2\hbar\omega_m}\right]\times\frac{g_1^2+\mathcal{Q}^2+g_1}{(1+g_1)(\mathcal{Q}^2+g_1)}+\frac{\gamma_m}{\pi\omega_m}\ln\left(\frac{\hbar\varpi}{2\pi kT}\right). \tag{41}$$

This expression coincides with the corresponding one obtained in [12] using a master-equation description, except for the logarithmic correction, which however, in the case of mirror with a good quality factor $\mathcal{Q}$, is quite small, even in the intermediate-temperature range $\hbar\varpi\gg k_BT\gg\hbar\omega_m$.

A peculiar aspect of the stochastic cooling feedback scheme, which has not been underlined in [12], is its capability of inducing steady-state correlations between the position and the momentum of the mirror, i.e., the fact that $\langle QP+PQ\rangle_{st}\neq 0$. This correlation can be evaluated in the same way as above, starting from Eqs. (17a) and (17b), and getting

$$\frac{\langle QP+PQ\rangle_{st}}{2}=-\int_0^\infty dt'\int_0^\infty dt''K_Q(t')\chi_{sc}(t'')c_1(t'-t'')+\int_0^\infty dt'\int_0^\infty dt''K_P(t')\chi_{sc}(t'')c_2(t'-t''). \tag{42}$$

Then, using Eqs. (18), (19), (20), and (31), and performing the classical approximation on the quantum Brownian motion contribution (there is no ultraviolet divergence for $\varpi\to\infty$ in this case), one gets

$$\frac{\langle QP+PQ\rangle_{st}}{2}=\left(\frac{\zeta}{8}+\frac{k_BT}{2\hbar\omega_m}\right)\frac{g_1\mathcal{Q}}{(1+g_1)(\mathcal{Q}^2+g_1)}-\frac{g_1^2}{8\eta\zeta}\frac{\mathcal{Q}}{(1+g_1)(\mathcal{Q}^2+g_1)}. \tag{43}$$

Each steady-state expression (36), (41), and (43) has three contributions: the thermal term due to the mirror Brownian motion, the back action of the radiation pressure, proportional to the input power ζ, and the feedback-induced noise term proportional to g_1^2 and inversely proportional to the input power. At sufficiently large temperatures, the thermal noise contribution is much larger than the others and the mirror dynamics is faithfully described in terms of *classical* stochastic equations. This classical description amounts to neglect all the radiation input noises into the evolution equations of the system, so that $\mathcal{W}(t)$ is the only noise acting on the system. This classical description has been successfully used in Refs. [11,15] to account for the experimental data, in the case of a cold damping feedback scheme at room temperature. It is, however, evident that the radiation back action and the feedback-induced noise cannot be neglected in general. For example, the classical approximation for $\langle Q^2\rangle_{st}$ suggests that it would be possible to localize the mirror without limit, i.e., $\langle Q^2\rangle_{st}\to 0$, using an ever increasing feedback gain g_1 and keeping the input power fixed, while this is no more true as soon as the feedback-induced noise term proportional to g_1^2 is included.

The stochastic cooling feedback scheme has been introduced in [12] as a promising method for significantly cooling the cavity mirror. Let us, therefore, consider the optimal conditions for cooling, and the cooling limits of this scheme. The interesting quantity is the stationary oscillator energy U_{st}, which, neglecting the logarithmic correction of Eq. (41), can be written as

$$U_{st}=\hbar\omega_m[\langle Q^2\rangle_{st}+\langle P^2\rangle_{st}]=\frac{\hbar\omega_m}{8}\left[\frac{g_1^2}{\eta\zeta}\frac{(1+2\mathcal{Q}^2+g_1)}{(1+g_1)(\mathcal{Q}^2+g_1)}+\left(\zeta+\frac{4k_BT}{\hbar\omega_m}\right)\frac{(g_1^2+2\mathcal{Q}^2+g_1)}{(1+g_1)(\mathcal{Q}^2+g_1)}\right]. \tag{44}$$

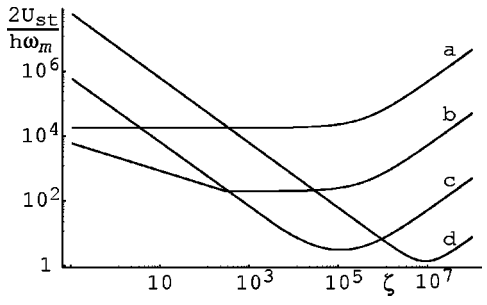

FIG. 2. Rescaled steady-state energy $2U_{st}/\hbar\omega_m$ versus the rescaled input power ζ, plotted for different values of g_1 (a: $g_1=10$, b: $g_1=10^3$, c: $g_1=10^5$, d: $g_1=10^7$) at fixed $\mathcal{Q}=10^7$, and with $k_BT/\hbar\omega_m=10^5$ and $\eta=0.8$. The optimal input power ζ_{opt} correspondingly increases, and for high gain values, ground-state cooling can be achieved.

It is evident from Eq. (44) that the effective temperature is decreased only if both $\mathcal{Q}$ and g_1 are very large. At the same time, the additional terms due to the feedback-induced noise and the back-action noise have to remain bounded for $\mathcal{Q}\rightarrow\infty$ and $g_1\rightarrow\infty$, and this can be obtained by minimizing U_{st} with respect to ζ keeping $\mathcal{Q}$ and g_1 fixed (physically this means optimizing the input power $\wp$ at given g_1 and $\mathcal{Q}$). It is possible to check that these additional terms are bounded only for very large $\mathcal{Q}$, that is, if $\mathcal{Q}/g_1\rightarrow\infty$ and in this case the minimizing rescaled input power is $\zeta_{opt}\simeq g_1/\sqrt{\eta}$. Under these conditions, the steady-state oscillator energy becomes

$$U_{st}\simeq\frac{\hbar\omega_m}{2}\left[\frac{1}{\sqrt{\eta}}+\frac{2k_BT}{\hbar\omega_m}\frac{1}{g_1}\right], \tag{45}$$

showing that, in the ideal limit $\eta=1$, $g_1\rightarrow\infty$, $\zeta\sim g_1\rightarrow\infty$, $\mathcal{Q}/g_1\rightarrow\infty$, the stochastic cooling feedback scheme is able to reach the quantum limit $U_{st}=\hbar\omega_m/2$, i.e., it is able to cool the mirror down to its quantum ground state. The behavior of the steady-state energy is shown in Figs. 2 and 3, where U_{st} (in zero-point energy units $\hbar\omega_m/2$) is plotted as a function of the rescaled input power ζ. In Fig. 2, $2U_{st}/\hbar\omega_m$ is plotted for increasing values of g_1 [(a) $g_1=10$, (b) $g_1=10^3$, (c) $g_1=10^5$, (d) $g_1=10^7$] at fixed $\mathcal{Q}=10^7$, and with $k_BT/\hbar\omega_m=10^5$ and $\eta=0.8$. The figure shows the corresponding increase of the optimal input power minimizing the energy, and

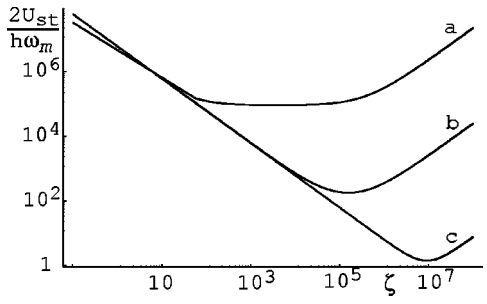

FIG. 3. Rescaled steady-state energy $2U_{st}/\hbar\omega_m$ versus ζ for increasing values of the mechanical quality factor $\mathcal{Q}$ (a: $\mathcal{Q}=10^3$, b: $\mathcal{Q}=10^5$, c: $\mathcal{Q}=10^7$) at fixed $g_1=10^7$, and with $k_BT/\hbar\omega_m=10^5$ and $\eta=0.8$.

that for high gain values, ground-state cooling can be essentially achieved, even with a nonunit detection efficiency. In Fig. 3, $2U_{st}/\hbar\omega_m$ is instead plotted for increasing values of the mechanical quality factor $\mathcal{Q}$ [(a) $\mathcal{Q}=10^3$, (b) $\mathcal{Q}=10^5$, (c) $\mathcal{Q}=10^7$] at fixed $g_1=10^7$. The figure clearly shows the importance of $\mathcal{Q}$ in stochastic cooling feedback and that ground-state cooling is achieved only when $\mathcal{Q}$ is sufficiently large.

The possibility to reach ground-state cooling of a macroscopic mirror using the feedback scheme of Ref. [12] was first pointed out, using an approximate treatment, in [35], where the need of a very large mechanical quality factor is underlined. Here we confirm this result using the more general QLE approach.

The steady state of the mirror mode in the presence of stochastic cooling feedback shows other peculiar aspects and interesting limiting cases. Thanks to the linearization of the problem [see Eqs. (7)], this steady state is a Gaussian state, which however is never exactly a thermal state because it is always $\langle Q^2\rangle_{st}\neq\langle P^2\rangle_{st}$ and $\langle QP+PQ\rangle_{st}\neq 0$. Its phase-space contours are therefore ellipses, rotated by an angle $\phi=(1/2)\arctan[\langle QP+PQ\rangle_{st}/(\langle Q^2\rangle_{st}-\langle P^2\rangle_{st})]$ with respect to the Q axis. The steady state becomes approximately a thermal state only in the limit of very large $\mathcal{Q}$ (and $\mathcal{Q}^2\gg g_1$), as it can be seen from Eqs. (36), (41), and (43). This thermal state approaches the quantum ground state of the oscillating mirror when also the feedback gain and the input power become very large. There are, however, other interesting limits in which the stochastic cooling feedback steady state shows nonclassical features. For example, the Gaussian steady state becomes a contractive state, which has been shown to be able to break the standard quantum limit in [36], when $\langle QP+PQ\rangle_{st}$ becomes negative, and this can be achieved at sufficiently large feedback gain, that is, when $g_1>\eta\zeta(\zeta+4k_BT/\hbar\omega_m)$ [see Eq. (43)]. Finally, stochastic cooling feedback can be used even to achieve steady-state position squeezing, that is, to beat the standard quantum limit $\langle Q^2\rangle_{st}<1/4$. The strategy is similar to that followed for cooling. First of all one has to minimize $\langle Q^2\rangle_{st}$ with respect to the input power ζ at fixed g_1 and $\mathcal{Q}$, obtaining

$$\langle Q^2\rangle_{st}^{min}=\frac{g_1\mathcal{Q}\sqrt{1+\mathcal{Q}^2+g_1}}{4\sqrt{\eta}(1+g_1)(\mathcal{Q}^2+g_1)}+\frac{k_BT}{2\hbar\omega_m}\frac{\mathcal{Q}^2}{(1+g_1)(\mathcal{Q}^2+g_1)}. \tag{46}$$

This quantity can become arbitrarily small in the limit of very large feedback gain, and provided that $g_1\gg\mathcal{Q}^2$. That is, differently from cooling, position squeezing is achieved in the limit $g_1\rightarrow\infty$ (implying $\zeta\rightarrow\infty$), and there is no condition on the mechanical quality factor. Under this limiting conditions, $\langle Q^2\rangle_{st}$ goes to zero as $g_1^{-1/2}$, and, at the same time, $\langle P^2\rangle_{st}$ diverges as $g_1^{3/2}$, so that, in this limit, the steady state for the stochastic cooling feedback approaches the position eigenstate with $Q=0$, that is, the mirror tends to be perfectly localized at its equilibrium position. The possibility to beat the standard quantum limit for the position uncertainty is

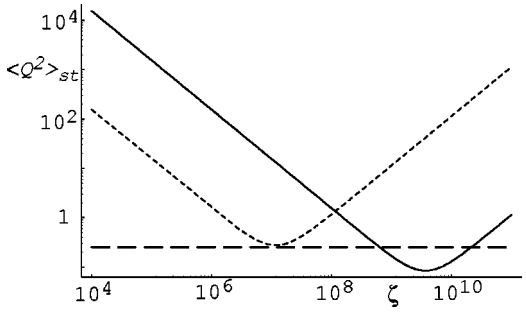

FIG. 4. Steady-state position variance $\langle Q^2 \rangle_{st}$ versus ζ for two values of the feedback gain, $g_1 = 10^7$ (dotted line), and $g_1 = 10^9$ (full line). The dashed line denotes the standard quantum limit $\langle Q^2 \rangle_{st} = 1/4$, while the other parameters are $\mathcal{Q} = 10^4$, $k_B T/\hbar\omega_m = 10^5$ and $\eta = 0.8$.

shown in Fig. 4, where $\langle Q^2 \rangle_{st}$ is plotted versus ζ for two different values of the feedback gain, $g_1 = 10^7$ (dotted line), and $g_1 = 10^9$ (full line), with $\mathcal{Q} = 10^4$, $k_B T/\hbar\omega_m = 10^5$, and $\eta = 0.8$. For the higher value of the feedback gain, the standard quantum limit $\langle Q^2 \rangle_{st} = 1/4$ (dashed line) is beaten in a range of values of the input power ζ.

B. Cold damping feedback

Now we characterize the stationary state of the mirror in the presence of cold damping. This stationary state has been already studied using classical arguments in [11,15], while the discussion of the cooling limits of cold damping in the quantum case has been recently presented in [18]. Here we shall generalize the results of [18] to the case of nonideal quantum efficiency $\eta < 1$, and we shall compare the cooling capabilities of the two feedback schemes.

Using the solution (25) for the time evolution, one has

$$\langle Q^2 \rangle_{st} = \lim_{t\to\infty} \langle Q(t)^2 \rangle = \int_0^\infty dt' \int_0^\infty dt'' \chi_{cd}(t') \chi_{cd}(t'') c(t'-t''), \quad (47)$$

where $c(t)$ is the stationary symmetrized correlation function of the noise term $n(t') = (2G\beta/\sqrt{\gamma_c}) X_{in}(t') + \mathcal{W}(t') - (g_{cd}/\sqrt{\gamma_c}) \dot{Y}_{in}(t') + (g_{cd}/2\sqrt{\gamma_c \eta}) \dot{Y}^{\eta}_{in}(t')$ appearing in Eq. (25). Using the correlation functions (3), (4), (13), and (24), one gets

$$c(t) = \frac{4G^2\beta^2}{\gamma_c} \delta(t) - \frac{g_{cd}^2}{4\eta\gamma_c} \ddot{\delta}(t) + \frac{\gamma_m}{2\pi\omega_m} \mathcal{F}_r(t). \quad (48)$$

Since in the cold damping case it is $P(t) = \dot{Q}(t)/\omega_m$, it is straightforward to derive from Eq. (47) the expressions for $\langle P^2 \rangle_{st}$ and $\langle PQ + QP \rangle_{st}$, which are given by

$$\langle PQ + QP \rangle_{st} = \frac{1}{\omega_m} \lim_{t\to\infty} \frac{d}{dt} \langle Q(t)^2 \rangle = 0, \quad (49)$$

$$\langle P^2 \rangle_{st} = \frac{1}{\omega_m^2} \int_0^\infty dt' \int_0^\infty dt'' \dot{\chi}_{cd}(t') \dot{\chi}_{cd}(t'') c(t'-t''). \quad (50)$$

These stationary expressions can be rewritten in terms of the Fourier transforms of the noise correlation functions, in the same way as we have done for the Brownian motion term in the preceding section. Using Eqs. (4), (26), (37), and (48), one has

$$\langle Q^2 \rangle_{st} = \gamma_m \int_{-\infty}^{\infty} \frac{d\omega}{2\pi} |\tilde{\chi}_{cd}(\omega)|^2 \left[\frac{\zeta}{4} + \frac{g_2^2}{4\eta\zeta} \frac{\omega^2}{\omega_m^2} \Theta_{\Delta\omega}(\omega) + \frac{\omega}{2\omega_m} \coth\left(\frac{\hbar\omega}{2k_B T} \right) \Theta_{[-\varpi,\varpi]}(\omega) \right], \quad (51)$$

$$\langle P^2 \rangle_{st} = \gamma_m \int_{-\infty}^{\infty} \frac{d\omega}{2\pi} \frac{\omega^2}{\omega_m^2} |\tilde{\chi}_{cd}(\omega)|^2 \left[\frac{\zeta}{4} + \frac{g_2^2}{4\eta\zeta} \frac{\omega^2}{\omega_m^2} \Theta_{\Delta\omega}(\omega) + \frac{\omega}{2\omega_m} \coth\left(\frac{\hbar\omega}{2k_B T} \right) \Theta_{[-\varpi,\varpi]}(\omega) \right], \quad (52)$$

where

$$\tilde{\chi}_{cd}(\omega) = \frac{\omega_m}{\omega_m^2 - \omega^2 + i\omega\gamma_m(1+g_2)} \quad (53)$$

is the frequency-dependent susceptibility of the mirror in the cold damping feedback scheme, and $\Theta_I(\omega)$ is a "gate" function, equal to 1 within the interval I and equal to zero outside. Notice that we have introduced not only the gate function $\Theta_{[-\varpi,\varpi]}(\omega)$ for the thermal noise term, but also the gate function $\Theta_{\Delta\omega}(\omega)$ for the feedback-induced noise term. In fact, it is easy to see that a frequency cutoff for the feedback is needed to avoid an ultraviolet divergence in the expression for $\langle P^2 \rangle_{st}$. Moreover, from an experimental point of view, any feedback loop is active only within a finite bandwidth, which in this case is given by $\Delta\omega$.

We first evaluate $\langle Q^2 \rangle_{st}$. The contribution of the feedback-induced term generally depends upon the value of the feedback bandwidth $\Delta\omega$. There are two relevant experimental situations: a narrow bandwidth containing the mechanical resonance peak, that is, $\gamma_m(1+g_2) < \Delta\omega < \omega_m$ (configuration used in Refs. [11,15]), or a wide bandwidth with a very large high-frequency cutoff $\varpi_{fb} \gg \omega_m$, $\gamma_m(1+g_2)$. However, since the factor $|\tilde{\chi}_{cd}(\omega)|^2$ in Eq. (51) is highly peaked around the resonance frequency ω_m, $\langle Q^2 \rangle_{st}$ is practically independent of the feedback loop bandwidth, as soon as $\gamma_m(1+g_2) < \Delta\omega$. In fact, either in the narrow bandwidth case, when the spectrum can be approximated by the constant term $g_2^2/4\eta\zeta$, or in the case of a very large cutoff frequency, when the ω^2 dependence is kept, one gets the same result for the feedback-induced contribution, because

$$\int_{-\infty}^{\infty}\frac{d\omega}{2\pi}\frac{\omega^2}{\omega_m^2}|\tilde{\chi}_{cd}(\omega)|^2=\int_{-\infty}^{\infty}\frac{d\omega}{2\pi}|\tilde{\chi}_{cd}(\omega)|^2 =\frac{1}{2\gamma_m(1+g_2)}. \tag{54}$$

For the Brownian motion contribution we have the same situation described in the stochastic cooling case: the exact expression is cumbersome [28], but in the commonly met condition $\hbar\omega_m \ll k_B T$, the classical approximation $\coth(\hbar\omega/2k_BT)\simeq 2k_BT/\hbar\omega$ can be made, and using Eq. (54) for both the thermal and the back-action contribution, one finally gets

$$\langle Q^2\rangle_{st}=\left[\frac{g_2^2}{8\eta\zeta}+\frac{\zeta}{8}+\frac{k_BT}{2\hbar\omega_m}\right]\frac{1}{1+g_2}. \tag{55}$$

Notice that the corresponding expression for the stochastic cooling feedback (36) coincides with Eq. (55) in the limit $\mathcal{Q}\gg 1, g_1$.

Differently from $\langle Q^2\rangle_{st}$, $\langle P^2\rangle_{st}$ depends upon the feedback loop bandwidth. In fact, in the large bandwidth case, the integrand in Eq. (52) tends to a constant at large frequencies, and in the limit of a very large cutoff frequency ϖ_{fb}, the feedback-induced contribution becomes

$$\langle P^2\rangle_{st}^{fb}=\frac{\gamma_m g_2^2}{8\eta\zeta}\frac{\varpi_{fb}}{\pi\omega_m^2}. \tag{56}$$

In the narrow bandwidth case instead, approximating the noise spectrum with the constant term $g_2^2/4\eta\zeta$, and using again Eq. (54) within Eq. (52), one gets a feedback-induced noise term contribution identical to that of $\langle Q^2\rangle_{st}$ of Eq. (55), which is independent of the feedback bandwidth.

A potential ultraviolet divergence and a dependence upon the frequency cutoff ϖ is present also in the quantum Brownian motion term. In fact, as we have seen in the preceding section, the classical expression for the thermal contribution to $\langle P^2\rangle_{st}$, holds only in the limit of very large temperatures, $k_BT\gg\hbar\varpi$, while, in the intermediate-temperature regime $\hbar\omega_m\ll k_BT\ll\hbar\varpi$, one has an additional logarithmic correction, so to get

$$\langle P^2\rangle_{st}^{BM}=\frac{k_BT}{2\hbar\omega_m}\frac{1}{1+g_2}+\frac{\gamma_m}{\pi\omega_m}\ln\left(\frac{\hbar\varpi}{2\pi kT}\right). \tag{57}$$

Finally, the back-action term is simply evaluated using Eq. (54) and one gets the same contribution as in Eq. (55),

$$\langle P^2\rangle_{st}^{ba}=\frac{\zeta}{8(1+g_2)}. \tag{58}$$

Therefore, the general expression for $\langle P^2\rangle_{st}$ depends on the parameter regime considered and it may generally depend upon the feedback loop high-frequency cutoff ϖ_{fb} and the thermal bath cutoff ϖ. However, in the common experimental situation of a narrow bandwidth around the resonance peak, $\gamma_m(1+g_2)<\Delta\omega<\omega_m$, and a high $\mathcal{Q}$ mechanical mode so that the logarithmic correction in Eq. (57) can be neglected, the dependence on the frequency cutoffs vanishes and one has $\langle P^2\rangle_{st}=\langle Q^2\rangle_{st}$. Therefore, under these conditions, since it is also $\langle QP+PQ\rangle_{st}=0$, the stationary state in the presence of the cold damping feedback scheme is an effective thermal state with a mean excitation number $\langle n\rangle=2\langle Q^2\rangle_{st}-1/2$, where $\langle Q^2\rangle_{st}$ is given by Eq. (55). This effective thermal equilibrium state in the presence of cold damping has been already pointed out in [11,15], within a classical treatment neglecting both the back-action and the feedback-induced terms. The present fully quantum analysis shows that cold damping has two opposite effects on the effective equilibrium temperature of the mechanical mode: on one hand T is reduced by the factor $(1+g_2)^{-1}$, but, on the other hand, the effective temperature is increased by the additional noise terms.

Let us now consider the optimal conditions for cooling and the cooling limits of the cold damping feedback scheme. In the narrow feedback loop bandwidth case, and neglecting the logarithmic correction to $\langle P^2\rangle_{st}^{BM}$, the stationary oscillator energy is given by

$$U_{st}=2\hbar\omega_m\langle Q^2\rangle_{st}=\frac{\hbar\omega_m}{4(1+g_2)}\left[\frac{g_2^2}{\eta\zeta}+\zeta+\frac{4k_BT}{\hbar\omega_m}\right]. \tag{59}$$

This expression coincides with that derived and discussed in [18], except for the presence of the homodyne detection efficiency η, which was ideally assumed equal to 1 in [18]. The optimal conditions for cooling can be derived in the same way as it has been done in [18]. The energy U_{st} is minimized with respect to ζ keeping g_2 fixed, thereby getting $\zeta_{opt}=g_2/\sqrt{\eta}$. Under these conditions, the stationary oscillator energy becomes

$$U_{st}=\frac{\hbar\omega_m}{2}\frac{g_2}{1+g_2}\left[\frac{1}{\sqrt{\eta}}+\frac{2k_BT}{\hbar\omega_m}\frac{1}{g_2}\right], \tag{60}$$

showing that, in the ideal limit $\eta=1$, $g_2\to\infty$ (and therefore $\zeta\sim g_2\to\infty$), also the cold damping scheme is able to reach the quantum limit $U_{st}=\hbar\omega_m/2$, i.e., it is able to cool the mirror to its quantum ground state, as first pointed out in [18]. However, differently from the stochastic cooling case of the preceding section, the stationary energy does not depend on the mechanical quality factor, implying that cooling is easier to achieve using cold damping, because the additional condition $\mathcal{Q}/g_2\to\infty$ is not necessary in this case. However, cold damping, at variance with stochastic cooling feedback, does not yield any nonclassical feature in the steady state. Figure 5 shows the rescaled steady-state energy $2U_{st}/\hbar\omega_m$ versus ζ plotted for increasing values of g_2 [(a) $g_2=10$, (b) $g_2=10^3$, (c) $g_2=10^5$, (d) $g_2=10^7$], with $k_BT/\hbar\omega_m=10^5$ and $\eta=0.8$. The figure is essentially indistinguishable from Fig. 2, since, as we have seen, the steady states for the two feedback schemes become identical for large mechanical quality factors. For high gain values, ground-state cooling can be achieved also in this case, even with nonunit homodyne detection efficiency.

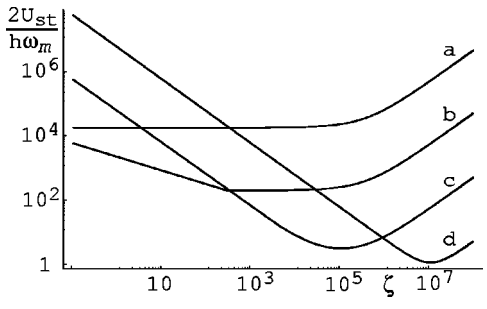

FIG. 5. Rescaled steady-state energy $2U_{st}/\hbar\omega_m$ versus the rescaled input power ζ, plotted for different values of g_2 (a: $g_2=10$, b: $g_2=10^3$, c: $g_2=10^5$, d: $g_2=10^7$), with $k_BT/\hbar\omega_m=10^5$ and $\eta=0.8$. The optimal input power correspondingly increases, and for high gain values, ground-state cooling can be achieved.

The ultimate quantum limit of ground-state cooling is achieved in both schemes only if *both* the input power and the feedback gain go to infinity. If instead the input power is kept fixed, the effective temperature does not decrease monotonically for increasing feedback gain, but, as it can be easily seen from Eqs. (44) and (59), there is an optimal feedback gain, giving a minimum steady-state energy, generally much greater than the quantum ground-state energy. The existence of an optimal feedback gain at fixed input power is a consequence of the feedback-induced noise term originating from the quantum input noise of the radiation. In a classical treatment neglecting all quantum radiation noises, one would have instead erroneously concluded that the oscillator energy can be made arbitrarily small, by increasing the feedback gain, and independently of the radiation input power. This is another example of the importance of including the radiation quantum noises, showing again that a full quantum treatment is necessary to get an exhaustive description of the system dynamics [16].

The experimental achievement of ground-state cooling via feedback is prohibitive with present day technology. For example, the experiments of Refs. [11,15] have used feedback gains up to $g_2=40$ and an input power corresponding to $\zeta\simeq 1$, and it is certainly difficult to realize in practice the limit of very large gains and input powers. This is not surprising, since this would imply the preparation of a mechanical macroscopic degree of freedom in its quantum ground state, which is remarkable. The same considerations hold for breaking the standard quantum limit for the steady-state position fluctuations with the stochastic cooling feedback.

V. SPECTRAL MEASUREMENTS AND THEIR SENSITIVITY

Both stochastic cooling and cold damping feedback schemes cool the mirror by overdamping it, thereby strongly decreasing its mechanical susceptibility at resonance [see Eqs. (34) and (53)]. As a consequence, the oscillator does not resonantly respond to the thermal noise, yielding in this way an almost complete suppression of the resonance peak in the noise power spectrum. Since the effective temperature is proportional to the area below the noise power spectrum, this implies cooling. However, the strong reduction of the mechanical susceptibility at resonance means that the mirror responds neither to the noise nor to any force acting on it. Therefore one expects that the SNR of the optomechanical device is not improved by feedback. However, we shall see that this intuitive guess is valid only under *stationary* conditions, and that, at least in the case of an *impulsive* force, a *nonstationary* strategy can be designed to improve the sensitivity for the detection of a weak classical force. The possibility to use the above feedback cooling schemes in a nonstationary way has been first shown in [16]. Here we shall reconsider and extend the treatment of [16], adopting a general description of nonstationary spectral measurements.

Spectral measurements are performed whenever the classical force $f(t)$ to detect has a characteristic frequency. Since the directly measured quantity is the output homodyne photocurrent $Y_{out}(t)$, we define the *signal* $S(\omega)$ as

$$S(\omega)=\left|\int_{-\infty}^{+\infty}dt e^{-i\omega t}\langle Y_{out}(t)\rangle F_{T_m}(t)\right|, \tag{61}$$

where $F_{T_m}(t)$ is a "filter" function, approximately equal to 1 in the time interval $[0,T_m]$ in which the spectral measurement is performed, and equal to zero otherwise. Using Eq. (11), the input-output relation (12), and the time evolution of the position operator $Q(t)$ [Eq. (17a) or (25)], the signal can be rewritten as

$$S(\omega)=\frac{8G\beta\eta}{2\pi\sqrt{\gamma_c}}\left|\int_{-\infty}^{+\infty}d\omega'\tilde{\chi}(\omega')\tilde{f}(\omega')\tilde{F}_{T_m}(\omega-\omega')\right|, \tag{62}$$

where $\tilde{f}(\omega)$ and $\tilde{F}_{T_m}(\omega)$ are the Fourier transforms of the force and of the filter function, respectively, and $\tilde{\chi}(\omega)$ is equal to $\tilde{\chi}_{sc}(\omega)$ or $\tilde{\chi}_{cd}(\omega)$, according to the feedback scheme considered.

The noise corresponding to the signal $S(\omega)$ will be given by its "variance"; since the signal is zero when $f(t)=0$, the noise spectrum can be generally written as

$$N(\omega)=\left\{\int_{-\infty}^{+\infty}dtF_{T_m}(t)\int_{-\infty}^{+\infty}dt'F_{T_m}(t')e^{-i\omega(t-t')}\times\langle Y_{out}(t)Y_{out}(t')\rangle_{f=0}\right\}^{1/2}, \tag{63}$$

where the subscript $f=0$ means evaluation in the absence of the external force. Using again Eqs. (11), (12), and the input noises correlation functions (3) and (13), the spectral noise can be rewritten as

$$N(\omega)=\left\{\frac{(8G\beta\eta)^2}{\gamma_c}\int_{-\infty}^{+\infty}dtF_{T_m}(t)\times\int_{-\infty}^{+\infty}dt'F_{T_m}(t')e^{-i\omega(t-t')}C(t,t')+\eta\int_{-\infty}^{+\infty}dtF_{T_m}(t)^2\right\}^{1/2}, \tag{64}$$

where $C(t,t')=\langle Q(t)Q(t')+Q(t')Q(t)\rangle/2$ is the symmetrized correlation function of the oscillator position. This very general expression of the noise spectrum is nonstationary because it depends upon the nonstationary correlation function $C(t,t')$. The last term in Eq. (64) is the shot noise term due to the radiation input noise.

Stationary spectral measurements

Spectral measurements are usually performed in the stationary case, that is, using a measurement time T_m much larger than the typical oscillator time scales. The most significant time scale is the mechanical relaxation time, which is γ_m^{-1} in the absence of feedback and $[\gamma_m(1+g_i)]^{-1}$ $(i=1,2)$ in the presence of feedback. In the stationary case, the oscillator is relaxed to equilibrium and, redefining $t'=t+\tau$, the correlation function $C(t,t')=C(t,t+\tau)$ in Eq. (64) is replaced by the *stationary* correlation function $C_{st}(\tau)=\lim_{t\to\infty}C(t,t+\tau)$. Moreover, for very large T_m, one has $F_{T_m}(t+\tau)\simeq F_{T_m}(t)\simeq 1$ and, defining the measurement time T_m so that $T_m=\int dt F_{T_m}(t)^2$, Eq. (64) assumes the form

$$N(\omega)=\left\{\left[\frac{(8G\beta\eta)^2}{\gamma_c}N_Q^2(\omega)+\eta\right]T_m\right\}^{1/2}, \tag{65}$$

where

$$N_Q^2(\omega)=\int_{-\infty}^{+\infty}d\tau e^{-i\omega\tau}C(\tau), \tag{66}$$

is the stationary position noise spectrum. This noise spectrum can be easily evaluated using the results of the preceding section. In fact, using the definition of $C_{st}(\tau)$ and the inverse Fourier transform of Eq. (66), one has

$$\langle Q^2\rangle_{st}=\lim_{t\to\infty}\langle Q^2(t)\rangle=C_{st}(0)=\int_{-\infty}^{+\infty}\frac{d\omega}{2\pi}N_Q^2(\omega). \tag{67}$$

The position noise spectrum can then be extracted from the stationary mean values derived in the preceding section. Using Eq. (51), one has

$$N_{Q,cd}^2(\omega)=\gamma_m|\tilde{\chi}_{cd}(\omega)|^2\left[\frac{\zeta}{4}+\frac{g_2^2}{4\eta\zeta}\frac{\omega^2}{\omega_m^2}\Theta_{\Delta\omega}(\omega)+\frac{\omega}{2\omega_m}\coth\left(\frac{\hbar\omega}{2k_BT}\right)\Theta_{[-\varpi,\varpi]}(\omega)\right], \tag{68}$$

for the cold damping scheme, while the derivation for the stochastic cooling case is less immediate. In fact, using Eqs. (30), (31), and (33), one gets

$$\langle Q^2\rangle_{st}=\int_{-\infty}^{+\infty}\frac{d\omega}{2\pi}\gamma_m\left[|\tilde{\chi}_{sc}(\omega)|^2\times\left(\frac{\zeta}{4}+\frac{\omega}{2\omega_m}\coth\left(\frac{\hbar\omega}{2k_BT}\right)\Theta_{[-\varpi,\varpi]}(\omega)\right)+|\tilde{K}_Q(\omega)|^2\frac{g_2^2}{4\eta\zeta}\Theta_{\Delta\omega}(\omega)\right]. \tag{69}$$

Then, using the Fourier transform of Eq. (19) in Eq. (69), one finally gets

$$N_{Q,sc}^2(\omega)=\gamma_m|\tilde{\chi}_{sc}(\omega)|^2\left[\frac{\zeta}{4}+\frac{g_2^2}{4\eta\zeta}\frac{\omega^2+\gamma_m^2}{\omega_m^2}\Theta_{\Delta\omega}(\omega)+\frac{\omega}{2\omega_m}\coth\left(\frac{\hbar\omega}{2k_BT}\right)\Theta_{[-\varpi,\varpi]}(\omega)\right]. \tag{70}$$

This position noise spectrum for the stochastic cooling feedback essentially coincides with that already obtained in [12], except that in that paper the high-temperature limit $[\coth(\hbar\omega/2k_BT)\simeq 2k_BT/\hbar\omega]$ is considered and the presence of the frequency cutoffs ϖ and ϖ_{fb} is not taken into account. The noise spectrum in the cold damping case of Eq. (68) instead essentially reproduces the one obtained in [18], with the difference that in Ref. [18] the homodyne detection efficiency η is set equal to 1, and the feedback and thermal noise cutoff functions have not been explicitly considered. The comparison between Eqs. (68) and (70) shows once again the similarities of the two schemes. The only differences lie in the different susceptibilities and in the feedback-induced noise term, which has an additional γ_m^2/ω_m^2 factor in the stochastic cooling case, which is, however, usually negligible with good mechanical quality factors. In fact, it is possible to see that the two noise spectra are practically indistinguishable in a very large parameter region.

The effectively detected position noise spectrum is not given by Eqs. (68) and (70), but one has to add the shot noise contribution due to the input noise in the homodyne photocurrent. In fact, using Eq. (65), and rescaling it to a position spectrum, one has

$$N_{Q,det}^2(\omega)=\gamma_m|\tilde{\chi}_i(\omega)|^2\left[\frac{\zeta}{4}+\frac{g_i^2}{4\eta\zeta}\frac{\omega^2+\delta_{i,1}\gamma_m^2}{\omega_m^2}+\frac{\omega}{2\omega_m}\coth\left(\frac{\hbar\omega}{2k_BT}\right)\right]+\frac{1}{4\eta\zeta\gamma_m}, \tag{71}$$

where $i=1$ refers to the stochastic cooling case and $i=2$ to the cold damping case. The homodyne-detected position noise spectrum is actually subject also to cavity filtering, yielding an experimental high-frequency cutoff γ_c, which however does not appear in Eq. (71) because we have adiabatically eliminated the cavity mode from the beginning. Therefore the spectrum of Eq. (71) provides a faithful description of the mirror mode dynamics only for $\omega<\gamma_c$; since it is usually $\varpi,\varpi_{fb}>\gamma_c$, we have not considered the feed-

back and reservoir cutoff functions in Eq. (71), and we shall not consider them in the following. The detected noise spectrum has three contributions: the Brownian motion term which is independent of the input power $\wp$, the shot noise term inversely proportional to $\wp$, and the back-action term, proportional to $\wp$. The main effect of feedback on the spectrum is the modification of the susceptibility due to the increase of damping, which is responsible for the suppression and widening of the resonance peak. This peak suppression in the noise spectrum has been already predicted and illustrated in [12,18], and experimentally verified for the cold damping case in [11,15]. Moreover, the feedback-induced noise term proportional to g_i^2 is responsible for an increase of the shot noise contribution to the spectrum. For a given feedback gain and frequency, the minimum noise is obtained at an intermediate, optimal, power, given by

$$\zeta_{opt}=\sqrt{\frac{1+\mathcal{Q}^{-2}g_i^2|\tilde{\chi}_i(\omega)|^2(\omega^2+\delta_{i,1}\gamma_m^2)}{\eta\gamma_m^2|\tilde{\chi}_i(\omega)|^2}}, \tag{72}$$

and the corresponding value of the minimum displacement noise is

$$N_{Q,min}^2(\omega)=\gamma_m|\tilde{\chi}_i(\omega)|^2\frac{\omega}{2\omega_m}\coth\left(\frac{\hbar\omega}{2k_BT}\right) + \frac{|\tilde{\chi}_i(\omega)|}{2\sqrt{\eta}}\sqrt{1+\mathcal{Q}^{-2}g_i^2|\tilde{\chi}_i(\omega)|^2(\omega^2+\delta_{i,1}\gamma_m^2)}. \tag{73}$$

This expression shows that both feedback schemes are able to arbitrarily reduce the displacement noise at resonance. In fact, using the fact that $\tilde{\chi}_i(\omega_m)\propto g_i^{-1}$ in both cases, one has that $N_{Q,min}^2(\omega_m)$ can be made arbitrarily small by increasing the feedback gain. This noise reduction at resonance is similar to that occurring to an oscillator with increasing damping, except that in our case, also the feedback-induced noise increases with the gain, and it can be kept small only if the input power is correspondingly increased in order to maintain the optimal condition (72). This arbitrary reduction of the position noise in a given frequency bandwidth with increasing feedback gain does not hold if the input power ζ is kept fixed. In this latter case, the noise has a frequency-dependent lower bound that cannot be overcome by increasing the gain. There is an important difference between the two feedback schemes. In fact, it is easy to check from Eq. (73) that in the cold damping case noise reduction takes place only close to resonance, and that the noise spectrum is not affected at lower frequencies [for example, $N_{Q,min}^2(\omega=0)$ is not changed by the cold damping feedback]. In the stochastic cooling case instead, frequency renormalization $\omega_m^2\rightarrow\omega_m^2+g_1\gamma_m^2$ allows one to reduce position noise even at low frequencies. This reduction of position noise out of resonance, without cold damping but with a feedback-induced increase of the mechanical frequency, has been demonstrated experimentally by Cohadon *et al.* in Ref. [11].

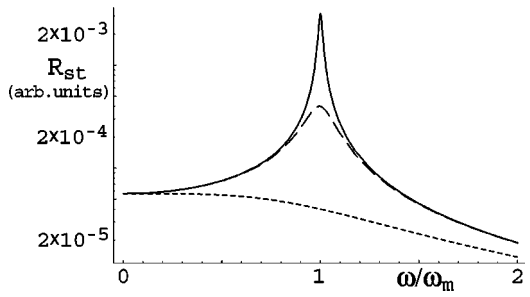

FIG. 6. Stationary SNR as a function of frequency in the case of an ideal impulsive force, i.e., $\tilde{f}(\omega)=$const. The full line refers to the case with no feedback, the dashed line to the case with $g_1=g_2=10^4$, and the dotted line to the case with $g_1=g_2=10^5$ (the two feedback schemes give indistinguishable results in these cases). The other parameters are $\mathcal{Q}=10^5$, $\zeta=10$, $k_BT/\hbar\omega_m=10^5$, and $\eta=0.8$. At a given frequency, the stationary SNR decreases for increasing feedback gain.

In the case of stationary spectral measurements also the expression of the signal simplifies. In fact, one has $\tilde{F}_{T_m}(\omega)\simeq\delta(\omega)$, and Eq. (62) assumes the traditional form

$$S(\omega)=\frac{8G\beta\eta}{2\pi\sqrt{\gamma_c}}|\tilde{\chi}(\omega)\tilde{f}(\omega)|. \tag{74}$$

The stationary SNR, $\mathcal{R}_{st}(\omega)$, is now simply obtained dividing the signal of Eq. (74) by the noise of Eq. (65),

$$\mathcal{R}_{st}(\omega)=|\tilde{f}(\omega)|\left\{\gamma_mT_m\left[\frac{\omega}{2\omega_m}\coth\left(\frac{\hbar\omega}{2k_BT}\right)+\frac{\zeta}{4} + \frac{1}{4\eta\zeta}\left(\frac{g_i^2}{\omega_m^2}(\omega^2+\delta_{i,1}\gamma_m^2)+\frac{1}{\gamma_m^2|\tilde{\chi}_i(\omega)|^2}\right)\right]\right\}^{-1/2}, \tag{75}$$

where again $i=1$ refers to the stochastic cooling case and $i=2$ to the cold damping case. It is easy to see that, in both cases, feedback *always lowers* the stationary SNR at any frequency, (except at $\omega=0$, where the SNR for the cold damping case does not depend upon the feedback gain). This is shown in Fig. 6, where the stationary SNR in the case of an ideal impulsive force [that is, $\tilde{f}(\omega)$ is a constant] is plotted for three values of the feedback gain. The curves refer to both feedback schemes because the two cases $i=1,2$ give always practically indistinguishable results, except for very low values of $\mathcal{Q}$. As mentioned at the beginning of the section, this result is not surprising because the main effect of feedback is to decrease the mechanical susceptibility at resonance, so that the oscillator is less sensitive not only to the noise but also to the signal. Therefore, even though the two feedback schemes are able to provide efficient cooling and noise reduction in narrow bandwidths for the mechanical mode, they cannot be used to improve the sensitivity of the optomechanical device for stationary measurements. In the following section we shall see how cooling via feedback can

be used to improve the sensitivity for the detection of impulsive forces, using an appropriate nonstationary strategy.

VI. HIGH-SENSITIVE NONSTATIONARY MEASUREMENTS

The two feedback schemes discussed here achieve noise reduction through a modification of the mechanical susceptibility. However, this modification does not translate into a sensitivity improvement because at the same time it strongly degrades the detection of the signal. The sensitivity of position measurements would be improved if the oscillator mode could keep its intrinsic susceptibility, unmodified by feedback, together with the reduced noise achieved by the feedback loop. This is obviously impossible in stationary conditions, but a situation very similar to this ideal one can be realized in the case of the detection of an *impulsive* force, that is, with a time duration σ much shorter than the mechanical relaxation time (in the absence of feedback), $\sigma \ll 1/\gamma_m$. In fact, one could use the following nonstationary strategy: prepare at $t=0$ the mirror mode in the cooled stationary state of Sec. IV, then suddenly turn off the feedback loop and perform the spectral measurement in the presence of the impulsive force for a time T_m, such that $\sigma \ll T_m \ll 1/\gamma_m$. In such a way, the force spectrum is still well reproduced, and the mechanical susceptibility is the one without feedback (even though modified by the short measurement time $T_m \ll 1/\gamma_m$). At the same time, the mechanical mode is far from equilibrium during the whole measurement, and its noise spectrum is different from the stationary form of Eq. (71), being mostly determined by the *cooled* initial state. As long as $T_m \ll \gamma_m$, heating, that is, the approach to the hotter equilibrium without feedback, will not affect and increase too much the noise spectrum. Therefore, one expects that as long as the measurement time is sufficiently short, the SNR for the detection of the impulsive force [which has now to be evaluated using the most general expressions (62) and (64)] can be significantly increased by this nonstationary strategy.

It is instructive to evaluate explicitly the nonstationary noise spectrum of Eq. (64) for the above measurement strategy. Let us first consider the cold damping case, which gives more compact expressions. Using Eq. (25), one gets

$$C(t,t') = K(t)K(t')\langle Q^2\rangle_{st} + \chi_0(t)\chi_0(t')\langle P^2\rangle_{st} + \int_0^t dt_1 \int_0^{t'} dt_2 \chi_0(t_1)\chi_0(t_2) c(t-t'-t_1+t_2), \tag{76}$$

where $\chi_0(t)$ is the mechanical susceptibility in the absence of feedback [see Eq. (34) with $g_1=0$ or Eq. (53) with $g_2=0$], $K(t)$ is given by Eq. (27) with χ_{cd} replaced by χ_0, $\langle Q^2\rangle_{st}$ and $\langle P^2\rangle_{st}$ are the stationary values in the presence of feedback evaluated in Sec. IV, and $c(t)$ is the cold damping noise correlation function introduced in Eqs. (47) and (48). This nonstationary correlation function has to be inserted in Eq. (64). Simple analytical results are obtained if we choose the following filter function:

$$F_{T_m}(t) = \theta(t) e^{-t/2T_m} \tag{77}$$

[$\theta(t)$ is the Heavyside step function], satisfying $\int dt F_{T_m}(t)^2 = T_m$. Using Eq. (77) and rewriting $c(t)$ in terms of its Fourier transform $\tilde{c}(\omega)$, one gets

$$N^2(\omega) = \frac{(8G\beta\eta)^2}{\gamma_c}\left[|\tilde{K}(\omega - i/2T_m)|^2 \langle Q^2\rangle_{st} + |\tilde{\chi}_0(\omega - i/2T_m)|^2 \langle P^2\rangle_{st} + |\tilde{\chi}_0(\omega - i/2T_m)|^2 \times \int_\infty^{+\infty} \frac{d\omega'}{2\pi} \frac{\tilde{c}(\omega')}{\frac{1}{4T_m^2} + (\omega'-\omega)^2} \right] + \eta T_m . \tag{78}$$

From Eq. (27), it is possible to see that $\tilde{K}(\omega) = (i\omega + \gamma_m)\tilde{\chi}_0(\omega)/\omega_m$; then, using Eq. (48) with $g_{cd}=0$, and the high-temperature approximation $\coth(\hbar\omega/2k_BT) \simeq 2k_BT/\hbar\omega$ for the Brownian noise, one finally gets the following expression for nonstationary noise spectrum for the cold damping feedback

$$N^2(\omega) = \frac{(8G\beta\eta)^2}{\gamma_c} |\tilde{\chi}_0(\omega - i/2T_m)|^2 \left[\frac{\omega^2 + (1/2T_m + \gamma_m)^2}{\omega_m^2} \times \langle Q^2\rangle_{st} + \langle P^2\rangle_{st} + \gamma_m T_m \left(\frac{\zeta}{4} + \frac{k_B T}{\hbar\omega_m} \right) \right] + \eta T_m . \tag{79}$$

The corresponding noise spectrum for the stochastic cooling case can be obtained in a similar way. Using Eq. (17a), one gets

$$C(t,t') = K_Q(t)K_Q(t')\langle Q^2\rangle_{st} + \chi_0(t)\chi_0(t')\langle P^2\rangle_{st} + [\chi_0(t)K_Q(t') + K_Q(t)\chi_0(t')] \frac{\langle QP+PQ\rangle_{st}}{2} + \int_0^t dt_1 \int_0^{t'} dt_2 \chi_0(t_1)\chi_0(t_2) c(t-t'-t_1+t_2), \tag{80}$$

where $K_Q(t)$ is given by Eq. (19) (with χ_{sc} replaced by χ_0), $\langle Q^2\rangle_{st}$, $\langle P^2\rangle_{st}$, and $\langle QP+PQ\rangle_{st}$ are the stationary values in the presence of stochastic cooling feedback evaluated in Sec. IV, and we have used the fact that, without feedback, $c_1(t)=0$ and $c_2(t)=c(t)$ [see Eqs. (31) and (48)]. Inserting this nonstationary correlation function in Eq. (64), using Eq. (77), the fact that $\tilde{K}_Q(\omega) = (i\omega + \gamma_m)\tilde{\chi}_0(\omega)/\omega_m$, and again the high-temperature approximation for the Brownian noise, one finally gets

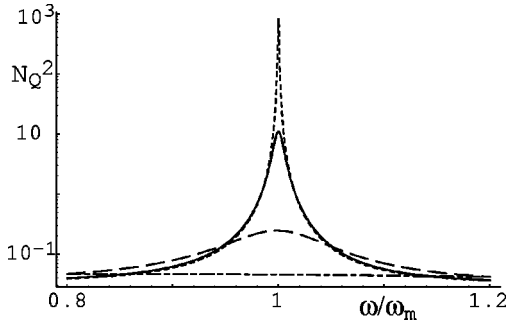

FIG. 7. Nonstationary noise spectrum $N_Q^2(\omega)=N^2(\omega_m)/4\eta\zeta\gamma_m T_m$ for different values of the measurement time, $\gamma_m T_m=10^{-1}$ (dotted line), $\gamma_m T_m=10^{-2}$ (full line), $\gamma_m T_m=10^{-3}$ (dashed line), $\gamma_m T_m=10^{-4}$ (dot-dashed line). The figure refers to the cold damping feedback scheme, but the curves are indistinguishable from those obtained with the stochastic cooling feedback, using the same parameters, $\mathcal{Q}=10^4$, $\zeta=10$, $g_1=g_2=10^3$, $k_BT/\hbar\omega_m=10^5$, $\eta=0.8$.

$$N^2(\omega)=\frac{(8G\beta\eta)^2}{\gamma_c}|\tilde{\chi}_0(\omega-i/2T_m)|^2 \times\left[\frac{\omega^2+(1/2T_m+\gamma_m)^2}{\omega_m^2}\langle Q^2\rangle_{st}+\langle P^2\rangle_{st} +\frac{\gamma_m+1/2T_m}{\omega_m}\langle QP+PQ\rangle_{st} +\gamma_m T_m\left(\frac{\zeta}{4}+\frac{k_BT}{\hbar\omega_m}\right)\right]+\eta T_m\,. \tag{81}$$

Notice that the two noise spectra (79) and (81) are very similar, the only difference being in the initial stationary values, whose explicit expression for the two feedback schemes is given in Sec. IV. It is also easy to check that the stationary noise spectrum corresponding to the situation with no feedback is recovered in the limit of large T_m, as expected, when the terms proportional to $\gamma_m T_m$ become dominant, and $\tilde{\chi}_0(\omega-i/2T_m)\to\tilde{\chi}_0(\omega)$. In the opposite limit of small T_m instead, the terms associated to the *cooled*, initial conditions are important, and since the terms proportional to $\gamma_m T_m$ are still small, this means having a reduced, nonstationary noise spectrum. This is clearly visible in Fig. 7, where the nonstationary noise spectrum, renormalized in order to have a position spectrum, $N_Q^2(\omega)=N^2(\omega)/4\eta\zeta\gamma_m T_m$, is plotted for different values of the measurement time T_m, $\gamma_m T_m=10^{-1}$ (dotted line), $\gamma_m T_m=10^{-2}$ (full line), $\gamma_m T_m=10^{-3}$ (dashed line), $\gamma_m T_m=10^{-4}$ (dot-dashed line). The resonance peak is significantly suppressed for decreasing T_m, even if it is simultaneously widened, so that one can even have a slight increase of noise out of resonance. This figure is referred to the cold damping feedback scheme, but it is indistinguishable from that obtained with the stochastic cooling feedback, using the same parameters ($\mathcal{Q}=10^4$, $\zeta=10$, $g_1=g_2=10^3$, $k_BT/\hbar\omega_m=10^5$, $\eta=0.8$). In fact, it can be checked that the two nonstationary noise spectra (79) and (81) differ significantly only at very low values of the mechanical quality factor ($\mathcal{Q}<10^2$). The effect of the terms depending upon the feedback-cooled initial conditions on the nonstationary noise is shown in Fig. 8, where the noise spectrum is plotted for different values of the feedback gain at a fixed value of T_m. In Fig. 8(a), $N_Q^2(\omega)$ is plotted at $\gamma_m T_m=10^{-3}$ for $g_2=1$ (full line), $g_2=10$ (dotted line), $g_2=10^2$ (dashed), $g_2=10^3$ (dot dashed). For this low value of $\gamma_m T_m$, the noise terms depending on the initial conditions are dominant, and increasing the feedback gain implies reducing the initial variances, and therefore an approximately uniform noise suppression at all frequencies. In Fig. 8b, $N_Q^2(\omega)$ is instead plotted at $\gamma_m T_m=10^{-1}$ for $g_2=1$ (full line), $g_2=10$ (dotted line), $g_2=10^2$ (dashed), $g_2=10^3$ (dot-dashed). In this case, the feedback-gain-independent, stationary terms become important, and the effect of feedback on the noise spectrum becomes negligible. Also in this case, Fig. 8 is valid for both stochastic cooling and cold damping schemes.

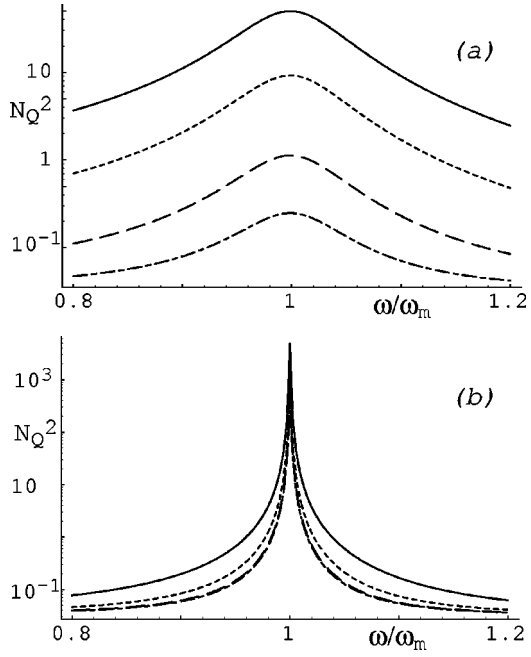

FIG. 8. Nonstationary noise spectrum $N_Q^2(\omega)$ for different values of the feedback gain, $g_2=1$ (full line), $g_2=10$ (dotted line), $g_2=10^2$ (dashed), $g_2=10^3$ (dot dashed), with fixed measurement time, $\gamma_m T_m=10^{-3}$ (a), and $\gamma_m T_m=10^{-1}$ (b). (a) corresponds to a strongly nonstationary condition, in which the noise is significantly suppressed, thanks to the cooled initial condition. In (b) the stationary terms becomes important and the noise reduction due to feedback cooling is less significant. The figure refers to the cold damping feedback scheme, but the curves are indistinguishable from those obtained with the stochastic cooling feedback, using the same parameters, $\mathcal{Q}=10^4$, $\zeta=10$, $k_BT/\hbar\omega_m=10^5$, $\eta=0.8$.

It is also possible to check from Eqs. (79) and (81) that, similarly to what happens for the stationary case, noise does not uniformly decrease for increasing feedback gain if the input power ζ is kept fixed, but there is an optimal feedback gain, minimizing the noise at a given frequency and input power.

The significant noise reduction attainable at short measurement times $\gamma_m T_m\ll 1$ is not only due to the feedback-

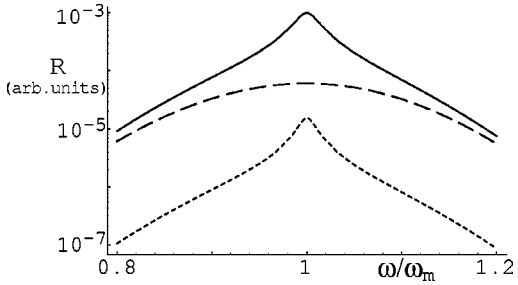

FIG. 9. Spectrum of the nonstationary SNR, $\mathcal{R}(\omega)$, with and without feedback cooling of the initial state. The full line refers to a nonstationary measurement, $\gamma_m T_m = 10^{-3}$, in the presence of feedback, $g = 2\times 10^3$ (the two feedback schemes give indistinguishable curves); the dashed line refers to the no-feedback case, and with the same, short, measurement time $\gamma_m T_m = 10^{-3}$. Finally, the dotted line refers to a "standard measurement," without feedback, and in the stationary limit $\gamma_m T_m = 10$. The other parameters are $\omega_f = \omega_m$, $\gamma_m \sigma = 10^{-4}$, $\gamma_m t_1 = 3\times 10^{-4}$, $\mathcal{Q} = 10^5$, $\zeta = 10$, $\eta = 0.8$, $k_B T/\hbar\omega_m = 10^5$.

cooled initial conditions, but it is also caused by the effective reduction of the mechanical susceptibility given by the short measurement time, $\tilde{\chi}_0(\omega) \to \tilde{\chi}_0(\omega - i/2T_m)$. This lowered susceptibility yields a simultaneous reduction of the signal at small measurement times $\gamma_m T_m \ll 1$, and therefore the behavior of the nonstationary SNR may be nontrivial. However, one expects that impulsive forces at least can be satisfactorily detected using a short measurement time, because the noise can be kept very small and the corresponding sensitivity increased. Let us check this fact considering the case of the impulsive force

$$f(t) = f_0 \exp[-(t-t_1)^2/2\sigma^2]\cos(\omega_f t), \tag{82}$$

where σ is the force duration, t_1 its "arrival time," and ω_f its carrier frequency. The corresponding SNR is obtained dividing the signal of Eq. (61), evaluated with Eq. (77), by the nonstationary noise spectra of Eqs. (79) and (81), and it is shown in Figs. 9 and 10. As anticipated, the sensitivity of the optomechanical device is improved using feedback in a nonstationary way. In Fig. 9, the spectral SNR, $\mathcal{R}(\omega)$, is plotted for different values of feedback gain and measurement time [as in the previous curves, the figures well describe both feedback schemes, because they give indistinguishable results for $\mathcal{R}(\omega)$ in the physically relevant parameter region]. The full line refers to $g_1 = g_2 = g = 2\times 10^3$ and $\gamma_m T_m = 10^{-3}$, the dashed line to the situation with no feedback and the same measurement time, $g = 0$ and $\gamma_m T_m = 10^{-3}$; finally the dotted line refers to a "standard" measurement, that is, no feedback and a stationary measurement, with a long measurement time, $\gamma_m T_m = 10$. The proposed nonstationary measurement scheme, "cool and measure," gives the highest sensitivity. This is confirmed also by Fig. 10, where the SNR at resonance, $\mathcal{R}(\omega_m)$, when feedback cooling is used with $g = 2\times 10^3$ (full line), and without feedback cooling (dotted line), is plotted as a function of the rescaled measurement time $\gamma_m T_m$. The preparation of the mirror in the cooled initial state yields a better sensitivity for any measurement time. As expected, the SNR in the presence of feedback approaches that without feedback in the stationary limit $\gamma_m T_m \gg 1$, when the effect of the initial cooling becomes irrelevant. Both Figs. 9 and 10 refer to a resonant ($\omega_f = \omega_m$) impulsive force with $\gamma_m \sigma = 10^{-4}$ and $\gamma_m t_1 = 3\times 10^{-4}$, while the other parameters are $\mathcal{Q} = 10^5$, $\zeta = 10$, $\eta = 0.8$, $k_B T/\hbar\omega_m = 10^5$.

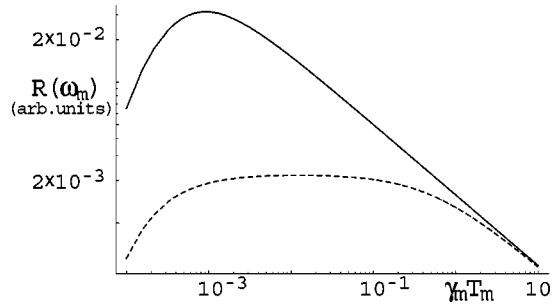

FIG. 10. Nonstationary SNR at resonance, $\mathcal{R}(\omega_m)$, with and without feedback cooling of the initial state, plotted as a function of the rescaled measurement time $\gamma_m T_m$. The full line refers to the case with feedback-cooled initial conditions ($g = 2\times 10^3$, the two feedback schemes give indistinguishable curves). The dotted line refers to the no-feedback case, $g = 0$. The other parameters are the same as in Fig. 9.

The proposed nonstationary strategy can be straightforwardly applied whenever the "arrival time" t_1 of the impulsive force is known: feedback has to be turned off just before the arrival of the force. However, the scheme can be easily adapted also to the case of an impulsive force with an *unknown arrival time*, as, for example, that of a gravitational wave passing through an interferometer. In this case it is convenient to repeat the process many times, i.e., subject the oscillator to cooling-heating cycles. Feedback is turned off for a time T_m during which the spectral measurement is performed and the oscillator starts heating up. Then feedback is turned on and the oscillator is cooled, and then the process is iterated. This cyclic cooling strategy improves the sensitivity of gravitational wave detection provided that the cooling time T_{cool}, which is of the order of $1/[\gamma_m(1+g_i)]$, is much smaller than T_m, which is verified at sufficiently large gains. Cyclic cooling has been proposed, in a qualitative way, to cool the violin modes of a gravitational waves interferometer in [15], and its capability of improving the high-sensitive detection of impulsive forces has been first shown in [16]. In the case of a random, uniformly distributed, arrival time t_1 and in the impulsive limit $\sigma \ll T_m$, the performance of the cyclic cooling scheme is well characterized by a time averaged SNR, i.e.,

$$\langle \mathcal{R}(\omega) \rangle = \frac{1}{T_m + T_{cool}} \left\{ \int_0^{T_m} dt_1 \mathcal{R}(\omega, t_1) + \int_{T_m}^{T_m + T_{cool}} dt_1 \mathcal{R}(\omega, t_1)_{cool} \right\}, \tag{83}$$

where $\mathcal{R}(\omega, t_1)$ is the nonstationary SNR at a given force arrival time t_1 discussed in this section, and $\mathcal{R}(\omega, t_1)_{cool}$ is

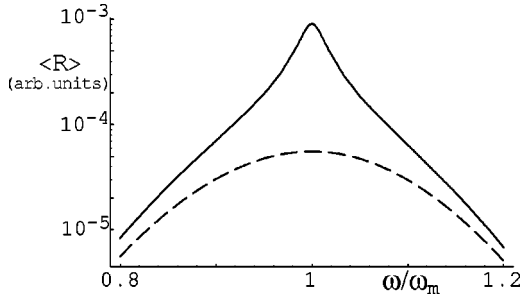

FIG. 11. Time averaged spectral SNR with and without cyclic cooling. The full line refers to cyclic cooling with $\gamma_m T_m = 10^{-3}$, $g = 2 \times 10^3$, and $T_{cool} = 10^{-3} T_m$ (the two feedback schemes give indistinguishable curves). The dashed line refers to the no-feedback case, with the same measurement time $\gamma_m T_m = 10^{-3}$ [see Eq. (85)]. The other parameters are $\omega_f = \omega_m$, $\gamma_m \sigma = 10^{-4}$, $\mathcal{Q} = 10^5$, $\zeta = 10$, $\eta = 0.8$, $k_B T / \hbar \omega_m = 10^5$.

the nonstationary SNR one has during the cooling cycle, which means with feedback turned on and with uncooled initial conditions. It is easy to understand that $\mathcal{R}(\omega, t_1)_{cool} \ll \mathcal{R}(\omega, t_1)$, and, since it is also $T_{cool} \ll T_m$, the second term in Eq. (83) can be neglected, so that [16]

$$\langle \mathcal{R}(\omega) \rangle \simeq \frac{1}{T_m + T_{cool}} \int_0^{T_m} dt_1 \mathcal{R}(\omega, t_1). \tag{84}$$

This time-averaged SNR can be significantly improved by cyclic cooling, as it is shown in Fig. 11, where $\langle \mathcal{R}(\omega) \rangle$ is plotted both with and without feedback. The full line describes the time-averaged SNR subject to cyclic feedback cooling with $g = 2 \times 10^3$, $\gamma_m T_m = 10^{-3}$, and $T_{cool} = 10^{-3} T_m$. In the absence of feedback, in the case of an impulsive force with unknown arrival time and duration σ, the best strategy is to perform repeated measurements of duration T_m without any cooling stage. The measurement time T_m can be optimized considering that it has to be longer than σ, and at the same time it has not to be too long, in order to have a good SNR (see the dotted line in Fig. 10). In this case, the time-averaged SNR can be written as

$$\langle \mathcal{R}_0(\omega) \rangle \simeq \frac{1}{T_m} \int_0^{T_m} dt_1 \mathcal{R}_0(\omega, t_1), \tag{85}$$

where $\mathcal{R}_0(\omega, t_1)$ is the SNR evaluated for $g = 0$. The dashed line in Fig. 11 refers to this case without feedback, and with $\gamma_m T_m = 10^{-3}$. The other parameter values are the same as in Figs. 9 and 10 and in this case, cyclic cooling provides an improvement at resonance by a factor 16 with respect to the case with no feedback. As suggested in Ref. [15], one could use nonstationary cyclic feedback to cool the violin modes in gravitational-wave interferometers, which have sharp resonances within the detection band. One expects that single gravitational bursts, having a duration smaller than the cooling cycle period, could be detected in this way.

VII. CONCLUSIONS

We have studied how quantum feedback schemes can be used to reduce thermal noise and improve the sensitivity of optomechanical devices. We have analyzed in detail the stochastic cooling scheme introduced in Ref. [12] and the cold damping scheme experimentally implemented in Refs. [11,15]. We have seen that the two schemes are physically analogous, even though they show some differences. In both cases, the main effect of feedback is the increase of mechanical damping, accompanied by the introduction of a controllable, measurement-induced, noise. The increase of damping means reduction of the susceptibility at resonance, and the consequent suppression of the resonance peak in the noise spectrum. Stochastic cooling feedback differs from cold damping in the fact that it has the supplementary effect of increasing the mechanical frequency. This means that, while cold damping achieves thermal noise reduction only around resonance, stochastic cooling is able to reduce noise even at very low frequencies, out of resonance. We have also shown that both schemes are able to achieve the ultimate quantum limit of ground-state cooling (see also [18] for the cold damping case). For both feedback schemes, ground-state cooling is reached in the limit of very large feedback gain, ideal homodyne detection, and very large input power. In the stochastic cooling case, however, also the additional condition of very large mechanical quality factor is needed (see also [35]), so that cooling is much more easily achieved in the cold damping case. In the limit of very large gain and input power, but with fixed mechanical quality factor, stochastic cooling feedback is instead able to achieve steady-state position squeezing, that is, one can beat the standard quantum limit $\langle Q_{st}^2 \rangle < 1/4$. Finally stochastic cooling is also able to produce stationary contractive states [36]. Reaching these quantum limits in optomechanical systems is experimentally very difficult but it would be extremely important, because it would be a genuine manifestation of quantum mechanics for a macroscopic mechanical degree of freedom.

We have also analyzed the sensitivity of the optomechanical device in the case of position spectral measurements for the detection of weak forces. Even though both feedback schemes are not able to improve the sensitivity of stationary measurements, we have shown how feedback can be used in a nonstationary way in order to increase the SNR in the case of impulsive forces. If the arrival time of the classical force is known, one has to keep the mirror mode cooled by feedback, and then turn off the feedback just before the arrival of the force. The mirror therefore responds to the force with its intrinsic susceptibility, not suppressed by the feedback, and with a nonstationary noise, reduced by the feedback. The SNR is increased as long as the measurement time T_m is longer than the force duration σ, but much smaller than the mechanical relaxation time, that is, $\sigma \ll T_m \ll 1/\gamma_m$. This nonstationary strategy can be well adapted to the case of a force with an unknown arrival time, for example, gravitational waves. In this case, the cooling and measurement steps have to be cyclically repeated (see also [15]), and the performance of cyclic cooling can be characterized by a SNR averaged over the force arrival time. This time-averaged SNR can be

significantly improved by cyclic cooling, thanks also to the fact that the cooling time can be made very small using very large feedback gains g, because it is $T_{cool} \simeq [\gamma_m(1+g)]^{-1}$. Different from ground-state cooling, the experimental implementation of these nonstationary strategy is feasible with current technology, and it may be useful not only for optomechanical devices, but also for microelectromechanical systems.

[1] C.M. Caves, Phys. Rev. Lett. **45**, 75 (1980); R. Loudon, *ibid.* **47**, 815 (1981); C.M. Caves, Phys. Rev. D **23**, 1693 (1981); P. Samphire, R. Loudon, and M. Babiker, Phys. Rev. **51**, 2726 (1995).

[2] J. Mertz, O. Marti, and J. Mlynek, Appl. Phys. Lett. **62**, 2344 (1993); T.D. Stowe, K. Yasamura, T.W. Kenny, D. Botkin, K. Wago, and D. Rugar, *ibid.* **71**, 288 (1997); G.J. Milburn, K. Jacobs, and D.F. Walls, Phys. Rev. A **50**, 5256 (1994).

[3] C.M. Caves, K.S. Thorne, R.W.P. Drever, V.D. Sandberg, and M. Zimmermann, Rev. Mod. Phys. **52**, 341 (1980).

[4] M.F. Bocko and R. Onofrio, Rev. Mod. Phys. **68**, 755 (1996).

[5] V.B. Braginsky, Zh. Eksp. Teor. Fiz. **53**, 1434 (1967) [Sov. Phys. JETP **26**, 831 (1968)].

[6] V.B. Braginsky and F. Ya Khalili, *Quantum Measurements* (Cambridge University Press, Cambridge, 1992).

[7] A. Abramovici *et al.* Science **256**, 325 (1992).

[8] Y. Hadjar, P.F. Cohadon, C.G. Aminoff, M. Pinard, and A. Heidmann, Europhys. Lett. **47**, 545 (1999).

[9] I. Tittonen, G. Breitenbach, T. Kalkbrenner, T. Müller, R. Conradt, S. Schiller, E. Steinsland, N. Blanc, and N.F. de Rooij, Phys. Rev. A **59**, 1038 (1999).

[10] I. Peterson, Sci. News (Washington, D. C.) **156**, 263 (1999).

[11] P.F. Cohadon, A. Heidmann, and M. Pinard, Phys. Rev. Lett. **83**, 3174 (1999).

[12] S. Mancini, D. Vitali, and P. Tombesi, Phys. Rev. Lett. **80**, 688 (1998).

[13] S. van der Meer, Rev. Mod. Phys. **57**, 689 (1985).

[14] J.M.W. Milatz and J.J. van Zolingen, Physica (Amsterdam) **19**, 181 (1953); J.M.W. Milatz, J.J. van Zolingen, and B.B. van Iperen, *ibid.* **19**, 195 (1953).

[15] M. Pinard, P.F. Cohadon, T. Briant, and A. Heidmann, Phys. Rev. A **63**, 013808 (2000).

[16] D. Vitali, S. Mancini, and P. Tombesi, Phys. Rev. A **64**, 051401(R) (2001).

[17] V. Giovannetti and D. Vitali, Phys. Rev. A **63**, 023812 (2001).

[18] J-M. Courty, A. Heidmann, and M. Pinard, Eur. Phys. J. D **17**, 399 (2001); see also e-print quant-ph/0107138.

[19] M.P. Blencowe and M.N. Wybourne, Physica B **280**, 555 (2000).

[20] A.N. Cleland and M.L. Roukes, Nature (London) **392**, 160 (1998).

[21] H.M. Wiseman, Phys. Rev. A **49**, 2133 (1994).

[22] V. Giovannetti, P. Tombesi, and D. Vitali, Phys. Rev. A **60**, 1549 (1999).

[23] M. Pinard, Y. Hadjar, and A. Heidmann, Eur. Phys. J. D **7**, 107 (1999).

[24] C.K. Law, Phys. Rev. A **51**, 2537 (1995).

[25] A.F. Pace, M.J. Collett, and D.F. Walls, Phys. Rev. A **47**, 3173 (1993); K. Jacobs, P. Tombesi, M.J. Collett, and D.F. Walls, *ibid.* **49**, 1961 (1994); S. Mancini and P. Tombesi, *ibid.* **49**, 4055 (1994).

[26] K. Jacobs, I. Tittonen, H.M. Wiseman, and S. Schiller Phys. Rev. A **60**, 538 (1999).

[27] C.W. Gardiner, *Quantum Noise* (Springer-Verlag, Berlin, 1991).

[28] H. Grabert, U. Weiss, and P. Talkner, Z. Phys. B: Condens. Matter **55**, 87 (1984).

[29] F. Haake and R. Reibold, Phys. Rev. A **32**, 2462 (1985).

[30] A. Dorsel, J.D. McCullen, P. Meystre, E. Vignes, and H. Walther, Phys. Rev. Lett. **51**, 1550 (1983); A. Gozzini, F. Maccarone, F. Mango, I. Longo, and S. Barbarino, J. Opt. Soc. Am. B **2**, 1841 (1985).

[31] H.M. Wiseman and G.J. Milburn, Phys. Rev. A **47**, 642 (1993).

[32] H.M. Wiseman and G.J. Milburn, Phys. Rev. Lett. **70**, 548 (1993).

[33] A.C. Doherty and K. Jacobs, Phys. Rev. A **60**, 2700 (1999); A.C. Doherty, S. Habib, K. Jacobs, H. Mabuchi, and S.M. Tan, *ibid.* **62**, 012105 (2000); A.C. Doherty, K. Jacobs, and G. Jungman, *ibid.* **63**, 062306 (2001).

[34] F. Grassia, J.M. Courty, S. Reynaud, and P. Touboul, Eur. Phys. J. D **8**, 101 (2000).

[35] R. Folman, J. Schmiedmayer, H. Ritsch, and D. Vitali Eur. Phys. J. D **13**, 93 (2001).

[36] H.P. Yuen, Phys. Rev. Lett. **51**, 719 (1983); M. Ozawa, *ibid.* **60**, 385 (1988).